FACULTEIT
BIO-INGENIEURSWETENSCHAPPEN

MICROPLASTICS IN SEAWATER

FATE AND REMOVAL POTENTIAL THROUGHOUT REVERSE OSMOSIS INSTALLATIONS

Word count: 28 459

Arne Saldi

Student ID: 01001481

Promotors: Prof. Dr. Colin Janssen
Dr. Ir. Marjolein Vanoppen

A dissertation submitted to Ghent University to obtain the degree of master in Bioscience Engineering: Environmental Technology.

Academic year: 2018 - 2019

UNIVERSITEIT
GENT

Gent, June 7, 2019

The promotors,

Prof. Dr. Colin Janssen
Dr. Ir. Marjolein Vanoppen

The author,

Arne Saldi

ACKNOWLEDGEMENTS

In the first place I would like to express my gratitude towards Marjolein. Your unbridled and infinite enthusiasm was an enormous inspiration to keep on trying, and to keep on trying again, during this project. You manage to keep close track of your students' work, from beginning to end, and you are immediately there whenever help is needed. All the support, surprise pop-ins, amusing chit-chat and food leftovers are very much appreciated.

Of course I would also like to thank Prof. Dr. Colin Janssen. Your passion for this topic and your expert guidance inspired me to focus on this subject and to make something out of it. Not only did you introduce us into the world of research within the faculty's laboratory walls, you also invited us along to other institutes and companies outside of the university. Such experiences are all an added value to the formation of young researchers and engineers, for which I am grateful.

Many thanks to all the colleagues in the Paint, Isofys and Ghentox departments who were always ready to help out or to give advice wherever necessary. Thank you to all the other thesis students in the laboratory with whom I shared the joys and sufferings of the final academic year at Ghent University.

Thank you to my brother and my friends for all the support. And, at last, I would like to direct some words of thanks to the two most wonderful people on this planet, my parents, who have always been incredibly supportive during this 9-year crusade through university halls. Without my parents' support, I would never have been able to reach the point where I find myself right now.

LIST OF ABBREVIATIONS

ATP	Adenosine Triphosphate
CA	Cellulose Amide
DDT	Dichlorodiphenyltrichloroethane
DMF	Dual Media Filtration
ED	Electrodialysis
EDR	Electrodialysis Reversal
EDL	Electric Double Layer
HDPE	High-Density Polyethylene
LDPE	Low-Density Polyethylene
LLDPE	Linear Low-Density Polyethylenee
MED	Multi-Effect Flash
MF	Microfiltration
MP	Microplastics
MSF	Multi-Stage Flash
NF	Nanofiltration
NP	Nanoplastic
PA	Polyamide
PAH	Polycyclic Aromatic Hydrocarbons
PE	Polyethylene
PET	Polyethylene Teraphthalate
POP	Persistent Organic Pollutant
PP	Polypropylene
PS	Polystyrene
PSD	Particle Size Distribution

PVA	Polyvinyl Alcohol
PVC	Polyvinylchloride
RO	Reverse Osmosis
SR	Sulphate Removal
SWRO	Seawater Reverse Osmosis
UF	Ultrafiltration
UNEP	United Nations Environmental Program
WWTP	Wastewater Treatment Plant

CONTENTS

SUMMARY

Microplastic (MP) particles are reported to be found across our planet, from our land's rivers and lakes into the seas. Even down in the remote and pristine Southern Ocean surrounding Antarctica, MP pollution has been observed. Research has already been exploring the consequences and the hazards of their presence on the health of aquatic ecosystems and individual organisms, including human health. Ingestion may lead to suffocation or starvation, while the plastic products themselves contain additives such as pigments or plasticizers which are released to the environment and lead to e.g. endocrine disrupting effects. The main challenge in this issue of MP pollution is the prevention of plastic waste entering the aquatic systems. However, at the same time, the pollution has become a global concern and its removal will have to be part of solving this widespread problem.

The basic idea of this research is to look into a process which treats seawater at high flow rates on a daily basis. Given the increasing scarcity of drinking water, there is a growing demand for desalination capacity where seawater is processed to drinking water. An increasingly dominant process is seawater reverse osmosis (SWRO), a membrane-based technology to physically separate salt molecules from the water. To allow decent operation, this membrane process requires various pretreatment steps which gradually purify the incoming seawater. The goal of this thesis is to describe the fate of MP, present in the intake seawater, throughout this pretreatment in SWRO installations and to assess their potential for removal from this system.

The experimental part allowed to identify the reject stream of a dual media filtration (DMF) unit as a hotspot for MP that enter the SWRO installations, while the microfiltration (MF) unit acts in the same way if it is not preceded by a DMF unit. This study demonstrates that the fate of MP in these two conventional pretreatment steps is similar: a very high removal efficiency from the incoming stream and a significant fraction is flushed out during the backwash procedure of these filtration units. As a result, the MP are concentrated in the reject stream after backwashing. A series of simulation calculations based on a broad range of parameters (e.g. ingoing MP concentration or plastics composition) indicates a removal potential from 0.3 kg up to 5 tonnes of MP on a yearly basis in a conventional large-scale SWRO installation.

NEDERLANDSE SAMENVATTING

Microplastic (MP) vervuiling wordt teruggevonden over de hele planeet, van in de rivieren en meren tot in de zeëen. Zelfs in de afgelegen en ongerepte Zuidelijk Oceaan die Antarctica omgeeft is er MP vervuiling geobserveerd. Wetenschappelijk onderzoek heeft zich al toegelegd op de gevolgen en de gevaren van MP op de gezondheid van aquatische ecosystemen en individuele organismen, waaronder ook de menselijke gezondheid. De inname van MP kan tot verstikking of uithongering leiden. Bovendien bevatten de plastic materialen zelf ook additieven zoals pigmenten of weekmakers die vrijgesteld worden in het milieu met bv. een verstoring van het hormoonsysteem tot gevolg. De grote uitdaging gerelateerd met MP vervuiling is uiteraard het voorkomen dat plastic afval in de aquatische systemen terechtkomt. Tegelijkertijd is de huidige vervuiling geëvolueerd tot een globale zorg en zal de verwijdering ervan ook een deel van de oplossing van dit wijdverspreide probleem moeten zijn.

Het uitgangspunt van dit onderzoek is om een proces dat dagelijks zeer grote hoeveelheden zeewater behandelt van naderbij te bekijken. Door de toenemende schaarste van drinkwater is er een groeiende vraag naar ontziltingscapaciteit die zeewater kan verwerken tot drinkbaar water. Een almaar populairder wordend proces hiervoor is omgekeerde osmose (RO, reverse osmosis), een membraan-gebaseerde technologie die de zoutmoleculen fysisch scheidt van het zeewater onder hoge druk. Om een degelijke werking van de membranen voor RO te verzekeren vereist dit proces verschillende voorbehandelingsstappen die het oorspronkelijke zeewater stapsgewijs opzuiveren vooraleer het naar de eigenlijke RO gestuurd wordt. Het doel van deze thesis is om het verloop van de MP, aanwezig in het opgepompte zeewater, te bestuderen doorheen deze voorbehandeling van RO installaties en om zo het potentieel voor hun verwijdering uit dit systeem te beschrijven.

Het experimentele luik laat toe om de afvalstroom van dubbelmedia filtratie (DMF) aan te wijzen als een hotspot voor de opgepompte MP, terwijl een microfilter (MF) zich op een gelijkaardige manier gedraagt als het niet voorafgegaan zou worden door een DMF. Deze studie toont aan dat het verloop van MP in deze twee conventionele voorbehandelingsstappen dezelfde is: langs de ene kant een zeer hoge verwijderingsefficiëntie en langs de andere kant wordt er een aanzienlijk deel van de ingaande MP uitgewassen tijdens de terugspoeling van deze filtratie-eenheden. Op die manier worden

de MP opgeconcentreerd in de afvalstroom na terugspoelen. Simulatieberekeningen op basis van een breed bereik van parameters (bv. MP concentratie of samenstelling van de ingaande MP) duidt op een verwijderingspotentieel van 0.3 kg tot 5 ton MP per jaar in een conventionele grootschalige zeewater RO installatie.

CHAPTER 1

INTRODUCTION

Microplastic (MP) pollution is a result of fragments of plastic products that reach aquatic environments, eventually ending up in the world's seas and oceans. Their hazardous effect on ecosystems and especially biota has already been studied by various authors and the MP pollution is emerging more and more as a worldwide environmental problem. At the same time, marine plastic pollution has grown over the years as a research topic in the academic world. Reports by policy makers such as the UN heighten the urgency to extend knowledge on the subject, especially of interest in the area of marine biology and environmental studies [1]. Barboza and Garcia (2015) [2] show an exclusively increasing trend for studies on MP in the marine environment between 2004 to 2014. These emerging studies appear to focus mainly on transport routes, environmental impacts, interaction of MP with other contaminants and the quantification and characterization of these microparticles. All in all, scientific research on the subject is still young and there are many questions left unanswered. Relatively absent in all this new research is knowledge on the vertical distribution of plastics in the water column and the possibilities for removal of MP when seawater is processed by industrial installations.

In ocean water, MP are typically widespread but in relatively low concentrations (2.1.2). This accounts for one of the major challenges in terms of MP pollution abatement: research is looking for cost-effective methods of detection, collection and removal of MP from the marine environment. Currently, removal mechanisms are lacking [3] and the sources bringing more MP into the ocean waters have not been cut off either.

This study will focus on the behaviour and fate of MP throughout desalination installations (2.2) and their potential for removal will be discussed. Desalination installations based on reverse osmosis (RO) process big volumes of seawater. During the process, all treated seawater passes a series of treatment steps. As a result, the MP present in the process stream will equally undergo these steps and will behave according to their physical properties, such as density, size or shape (2.1.3).

Therefore, this study will explore the behaviour of plastic microparticles during these processes and, based on literature research and experimental research, predict and

discuss the potential for removal of the MP particles from these process streams. Now, these MP pass through such installations daily and little is known about how much plastic is treated and where it ends up in the system.

CHAPTER 2

LITERATURE REVIEW

2.1 Microplastics

2.1.1 Plastic Production

The production of plastics originates from the modification of natural materials, such as rubber or nitrocellulose. Eventually, from the start of the 20^{th} century onward, completely synthetic molecules were produced to mimic and further exploit the mechanical properties of these polymers (bakelite, polyvinyl chloride, polyethylene, etc.) [4]. By now, the use of plastics is widespread and it has become an integral part of people's lives. The development of plastic polymers has offered our society many benefits, ranging from the healthcare industry to transport and the food industry. Depending on the source, the worldwide production of plastics amounts to 385 million tonnes in 2015 [5] and continues to rise, as shown in Figure 2.1. Densely populated or industrialised areas logically form the main land-based source of plastic pollution to the ocean water bodies [6]. Typically cited activities that are sources of MP pollution are plastic bag usage [7], coastal recreation [8], wastewater effluent [9] and fishery [6].

Plastic material is a typically durable and versatile material and the diversity of available polymers offers a very large range of applications, from soft LLDPE (linear low-density polyethylene) foils to PVC (polyvinylchloride) piping. However, as a result of this durability and since a lot of these polymer products are not collected at their end-of-life stage, the pollution of plastics is also widespread. In 2016, the United Nations Environmental Program (UNEP) dedicated a copious report to the presence of plastic debris and MP in the marine environment, acknowledging the extent of this environmental problem and encouraging initiatives and policy changes in order to take on this issue. In the end, plastic litter in the ocean is considered a "common concern of humankind" [10].

Plastic materials are polymers chemically synthesised as a concatenation of a basic brick molecule, the monomer. There are hundreds of different types of polymers and

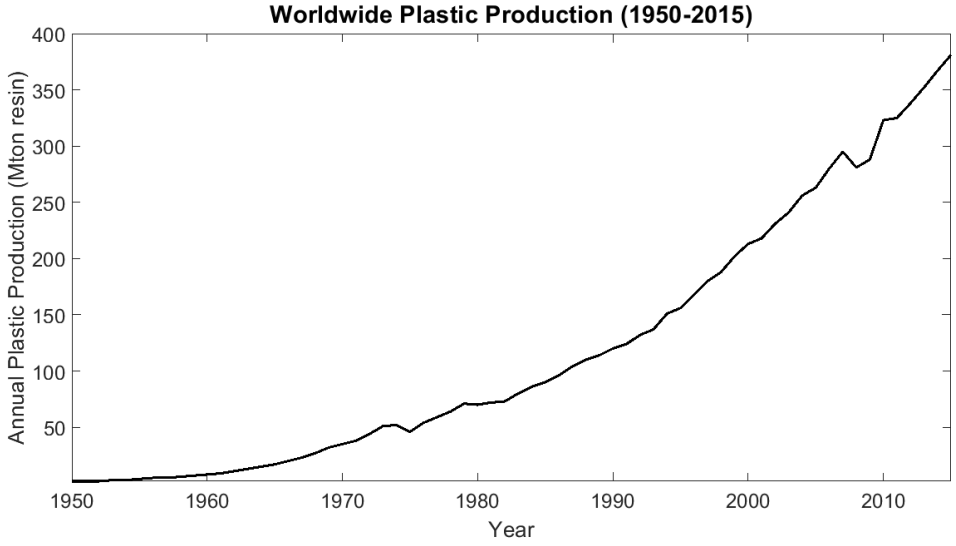

Figure 2.1: *The worldwide plastic production expressed as annual production (in million tonnes) from 1950 to 2015. Plastic production before 1950 can be considered negligible. (Own figure, data from Geyer et al. (2017) [5])*

each type has its own properties. This diversity allows for plastic materials to be very versatile and suitable for a multitude of applications. One major domain that is being dominated by plastic polymers is the packaging industry. Polymers are typically a low cost material, bio-inert and light weight, making them particularly suitable to replace materials such as glass or paper [1]. However, its low cost makes it less valuable to recycle and many packaging plastics are designed for single-use and contribute heavily to the worldwide plastic pollution. Table 2.1 lists the most commonly produced polymer types and some typical everyday applications. Most types of plastics consist of low-density or high-density polyethylene (LDPE and HDPE), or polypropylene (PP). As a result, these polymers are also expected to make up the greatest fraction of MP pollution. More specific, as is also suggested in Andrady (2011) [1], the assumption is made that the polymer type distribution of the original incoming MP pollution in oceans and seas is likely to reflect the worldwide production as shown in Table 2.1.

2.1.2 Microplastics in the marine environment

MP are plastic particles in the size range of 1 μm to 5 mm, however the lower boundary is unclear as it is usually set as the mesh size of sampling methods commonly used [3]. Research during the past decades has well established the presence of MP in the world's oceans [6, 11, 12], marine sediments [13, 14] and freshwater bodies [15, 16]. Concentrations for the water column, as reported in research studies, are usually in the magnitude of 0.1-10 particles/m^3, with the highest concentrations typically observed in the estuary areas and close to coastlines [6, 11, 12]. In a recent risk assessment study, Everaert et al. [17] predict a 50-fold increase of the MP pollution in

Table 2.1:
Overview of the most common polymer types, including their densities and annual production, expressed as percentage of the total worldwide plastics production. PP = polypropylene, LDPE = low-density polyethylene, HDPE = high-density polyethylene, PS = polystyrene, PA = polyamide (nylon), PET = polyethylene therephthalate, PVA = polyvinyl alcohol, CA = cellulose amide, PVC = polyvinyl chloride. PA's annual production was reported as <3%, CA's and PVA's was not mentioned but assumed 1.5%, in order to add up to 100% for the sake of future calculations. [1]

Polymer	Density Range [g/cm^3]	Average Density [g/cm^3]	Annual Production [%]	Applications
PP	[0.89, 0.91]	0.900	24	Bottle caps, netting
LDPE	[0.91, 0.94]	0.925	21	Plastic bags, straws
HDPE	[0.93, 0.98]	0.955	17	Milk jugs
PS	[1.04, 1.11]	1.075	6	Food containers, Foam cups
PA	[1.13, 1.15]	1.140	3	Netting, traps
PET	[1.19, 1.35]	1.270	7	Bottles
PVA	[1.19, 1.35]	1.270	1.5	Glue, Plaster
CA	[1.27, 1.34]	1.305	1.5	Cigarette filters
PVC	[1.20, 1.45]	1.325	19	Cups, Bottles, Plastic Film

terms of mass by 2100, reporting calculations of 9.6 to 48.8 particles/m^3, respectively a best-case and a worst-case scenario. However, most of the datasets cited in these studies are limited to the larger fraction of MP. However, in Li et al. (2016) [6], for example, only 2 of 26 included studies report their findings with a size range down to 50 μm and in a relevant concentration unit (particles/m^3). This still excludes an important fraction of the MP size range, especially when results are expressed based on number of particles. Studies point to a higher number-based frequency of smaller particles [18, 19]. In fact, these 2 studies mentioned in Li et al. (2016) [6] report concentrations of 4 594 and 16 000 particles/m^3, respectively [20] and [21], which is considerably higher when compared to other reported values. This goes to show that the sampling method plays a crucial role in investigating the extent of the pollution of MP in oceans and seas.

This research challenge is in line with another assumption, also proposed in Everaert et al. [17]. It is based on the fact that researchers usually do not include a lower limit for MP. As mentioned above, the lower limit of the MP size range is typically set in accordance with the sampling method and has become a loose and arbitrary border. As an example, in Desforges et al. (2014) [20], a sieve down to 62.5 μm is used, while in many other on-sea sampling campaigns neuston trawling nets with pore sizes from 150 μm [19] over 200 μm [18] to 330 μm [22] are used, for example. Like this, the selection of sampling device or method might automatically exclude smaller plastic fragments, such as nanoplastics (NP) and even the smaller fraction

of MP, which represent a much smaller pollution on mass basis but not on number basis and in terms of ecological threat. However, studies rarely focus on this form of pollution. Therefore, it can be assumed that measurements and research on MP underestimate the total pollution by plastics when the sampling method's lower size limit excludes a certain fraction of MP.

Typically, two types of MP are defined: primary MP and secondary MP. The first group consists of MP that are introduced directly into the ocean. On the one hand they are engineered as micromaterial for application in consumer products, such as cosmetics, paints or cleaning agents [23]. On the other hand, MP are also released directly by means of ship-breaking or via industrial abrasives [1]. However, it is suggested that the majority of plastic microfragments in the marine environment are due to the degradation of plastic litter in the oceans. These are categorised as secondary MP. Typically, photodegradation is the first degeneration step, usually followed by thermooxidative degeneration, i.e. slow oxidation of the molecules, and/or biodegradation [1].

The widespread pollution of MP has various consequences on individual organisms and ecosystems. The threats of MP can be discussed based on three categories: the particles themselves are a) a physical hazard, b) the particles can act as a vector for alien species, the biological hazard, and c) the presence of other products (e.g. plasticizers or coatings) associated with MP particles constitutes a chemical hazard.

a) The **physical hazard** includes the ingestion of MP particles by individual organisms. An important consequence of this ingestion is weight loss and starvation of individuals as they stop eating with a permanently filled stomach as the plastic particles are not broken down by the digestive system of the animal. Other biological effects are the onset of oxidative stress, the inhibition of photosynthesis in plankton and the occurrence of inflammatory reactions in tissues [11]. These phenomena have been well documented for e.g. fish [24], benthic species, [25, 26] sea birds [27, 28] and commercial species for human consumption, such as mussels and shrimps [11]. Additionally, organisms that have ingested MP, are also shown to fragment the particles in their digestive system, leading to an increase in smaller MP which can be excreted by the organisms. This suggests that higher animals, such as fish and birds, act as biovectors of MP particles to more remote oceanic regions [27]. These findings support the studied widespread character of MP pollution and its impact on ecosystems on a large spatial scale [1].

b) The **biological hazard** is the consequence of the emergence of MP as a new solid area on which marine microorganisms can grow. This growth has been characterized in many studies and it is shown that the bacterial community can be

very diverse and significantly different from communities as they occur in seawater [29]. As a result, the plastic particle acts as a freely moving vector of specific microbial communities which may lead to species dispersal and the introduction of alien species in ecosystems. Additionally, the biological activity of microorganisms on the polymer surface may lead to a higher leaching rate of additives present in the plastic particle, contributing to the chemical hazard as well [11]. The concept of biofouling of MP comes forward in many studies on MP and it is an important characteristic, not only in terms of an ecological opportunity or threat, but also in terms of the behaviour of the colonised particles themselves [30–33], which will be discussed later.

c) The **chemical hazard** associated with MP pollution originates from different classes of products. First of all, plastics contain various low-molecular additives next to their main structure of polymer chains [4]. Additives commonly encountered include phtalates and bisphenol A. These are used as plasticiser (main compound and auxiliary compound, respectively) in order to make the polymers easier to process. These additives (up to 50% of the end product [3]) have been shown to lead to endocrine disruption in organisms as they mimic or disrupt endogenous hormones [11]. Secondly, persistent organic pollutants (POPs) present at low concentrations in seawater can sorb onto the particle's surface. The equilibrium distribution coefficient K for common POPs ranges from 10^3 to 10^5 L/kg towards sorption on plastic particles in a plastic-water system [3]. This leads to an increase of their concentration by different orders of magnitude [24]. Examples of such POPs are polycyclic aromatic hydrocarbons (PAHs), chlorinated benzenes and DDT [11] and they are typically toxic to humans and wildlife in natural concentrations [34]. In this way, MP act as a vector of these POPs that spreads them throughout marine ecosystems. Also, both the plastics' additives and the concentrated POPs can enter an organism after ingestion of an MP particle, forming an additional toxicological pathway associated with MP pollution [11]. The actual release of these adsorbed chemical from the plastic particles into the organism's tissues has been investigated by thermodynamical modelling [35] and laboratory tests [36]. Field research on sea birds showed detection of brominated synthetic compounds that were not found in the birds' prey, however the same compounds were found after analysis of the MP present in the birds' stomachs [28].

2.1.3 Microplastic properties, biofouling and behaviour

There are various properties of MP that define their fate once released into seas and oceans. Certain particles are bound to stay afloat for a long time, others are assumed

to reside somewhere in the water column for long and, finally, others will quickly sink to the bottom and settle as part of the sea floor sediment. The most important defining properties are the particle's polymer type, density, rise velocity and size. The polymer type, by consequence, defines the particle's original density and its hydrophobic attributes, which will play a role in their initial behaviour in the seawater. The MP's size is an important parameter that also influences the particle's buoyancy in a certain medium as well as the rise velocity. The rise velocity is defined by the necessary time for a particle to cover a certain vertical distance, which can be positive (rising particle) or negative (sinking particle). A perfectly spherical particle, for example, is hindered less by drag forces than an irregularly shaped particle and will, by consequence, have a higher rise velocity.

The particle size is also related to the degree of biofouling that is possible and the influence of this biofouling on the final behaviour of a particle. A fundamental paper on mechanical characteristics of biofilms report a wet density of 1.14 g/cm^3 of biofilms [37], which is higher than seawater density. The average diameter of a bacterial cell is reported to be in the magnitude of μm, so an MP particle of 10 μm will be affected more by the attachment of a bacterial cell of a certain density than a particle of 5 mm [38]. As mentioned above, the plastic surface is an interesting surface on which microorganisms are likely to attach. Zettler et al. (2013) [29] describe their findings on colonisation of microorganisms on plastic debris collected from the top layer of open sea, coining these ecosystems the "Plastisphere". The identified organisms were very specific and the colonisation revealed significant differences with respect to what is found in the seawater surrounding the plastic particles. In their analyses, surface coverage by biomass amounted up to 8%.

As a result of the above factors, the vertical behaviour of MP in ocean waters can vary strongly and it cannot be simplified to a floating fraction of a density lower relative to the density of seawater and a settling fraction of higher density. In Law et al. (2010) [39], the authors report their findings on one of the notorious plastic gyres. A relatively constant amount of floating MP of particularly low density (mainly PP, LDPE and HDPE) is described over the years, even though, as can be seen in Figure 2.1, plastic production grows yearly. Therefore, it was already assumed that these lighter plastic fragments eventually sink below the surface as well. At the same time, studies indicate that most plastic particles found in sea sediments are of higher density than seawater [40]. This has led to the largely unanswered hypothesis of 'lost' plastics throughout the vertical water column. In previous studies, the vertical behaviour of MP particles has already been studied and linked to various properties. Reisser et al. (2015) [19] describe the faster vertical mixing of smaller floating particles compared to bigger particles, leading to an observed larger vertical decay of the

presence of MP based on mass rather than on number. Also, Kooi et al. (2017) [38] constructed a model to study the vertical distribution in the water column and the effect of biofouling on this behaviour. Positively buoyant particles exposed to marine biofouling conditions, such as light and oxygen, are prone to develop a biofilm aggregate on their surface, changing its properties as a whole. This is assumed to lead to a higher density in such a way that the particles might start sinking down. However, defouling due to grazing and light deficiency [41] supposedly leads to a vertical oscillatory pattern and a long residence time throughout the water column [38].

2.2 Seawater Desalination

2.2.1 Desalination

The depletion of water and drinking water resources is a major environmental challenge. Various regions are already faced with an increased drought and the demand for drinking water grows. One option to access a source of drinking water is the desalination of seawater. On average, seawater contains about 35 grams of salt per litre and it can be as high as 40 g/L [42, 43]. In order to produce drinking water, these salts need to removed together with other contaminants such as organic matter, microorganisms and particulate matter. There are two main technologies for desalination; thermal and membrane-based. Among these, various technologies are available. Examples for thermal desalination are multi-stage flash (MSF) and multi-effect flash (MED), membrane-based techniques are for example electrodialysis (ED) and reverse osmosis (RO). Over the last three decades, crucial improvements in RO technology have launched RO membranes as the go-to option for new desalination installations, meaning membrane-based desalination has taken over thermal desalination [44]. Only in the Middle East thermal desalination is still prominently present given the low cost of fossil fuels and the bad quality of seawater, hampering the applicability of membranes. Currently, the total desalination capacity reaches 90 million m^3/d [45]. As can be seen in Figure 2.2, RO comprises more than half of the desalination plants worldwide [46]. Despite its high energy demand, this is a growing technology and RO plants are surging. Especially in areas close to sea, close to a high energy supply and with little access to other drinking water sources, RO is technology gaining popularity.

Naturally, during desalination processes, large fluxes of seawater are taken up and pass through the system in order to separate particles and dissolved molecules from the seawater stream. A pure water stream is the end product of the entire process.

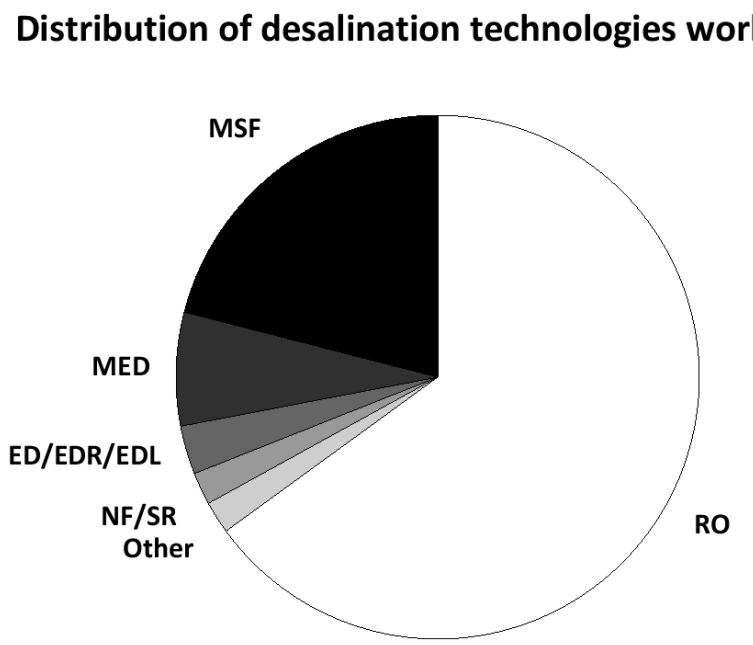

Figure 2.2: *An overview of the worldwide distribution of desalination technologies. RO = Reverse Osmosis; MSF = Multi-Stage Flash; MED = Multi-Effect Distillation; ED = Electrodialysis; EDR = Electrodialysis Reversal; EDL = Electric Double Layer; NF/SR = Nanofiltration/Sulphate Removal. (Own figure, data from GWI (2012) [45])*

However, there are also some waste streams (rejects) created throughout the system, which are typically being sent back to the source (e.g. sea or ocean), with post treatment if necessary. In this way, a potential flux of plastic particles passes through such desalination systems as well, which offers an opportunity for the removal of MP from seawater. Before focussing on this opportunity, the typical layout of seawater reverse osmosis (SWRO) plants is described which will play a central role in this study.

2.2.2 Reverse Osmosis

RO is a membrane technology where a water stream under high pressure (up to 60 bars [47]) is forced through a semi-permeable membrane: the water is able to pass through the filter while particulates and dissolved salts are rejected with a rejection of up to 99% [48]. The efficiency of RO is typically around 50 %. This means that half of the incoming water is purified while the other half of the stream is a reject stream containing the removed particles and salt molecules. The cut-off size of the RO modules is very small (less than 1 nm [46]) resulting in a high sensitivity to fouling, leading to an inoperable system due to too high pressure drops, or even irreversible fouling due to the presence of suspended solids [46]. Therefore, the seawater sent to the RO membrane modules requires pretreatment steps to allow a favourable operation.

Typical pretreatment can consist of screening, coagulation-flocculation, multi-media filtration [43], activated carbon modules, microfiltration (MF), etc. [46].

2.2.3 RO Pretreatment

Table 2.2 offers an overview of some large-scale SWRO installations worldwide. This non-exhaustive inventory of SWRO plants shows that the combination of dual medial filtration (DMF) and microfiltration (MF) is a common way to pretreat the incoming seawater before it is sent to the RO membranes. The coagulation-flocculation stage also appears frequently in these pretreatment lines. The capacity of the presented installations is higher than 50 000 m^3/d, which implies that they take in at least the double of this value as RO membranes typically show a recovery rate of about 50% (cfr. above in Section 2.2.2). DMF, mostly coupled with coagulation and flocculation to condition the incoming seawater, is a typical pretreatment for seawater streams and its main goal is the removal of coarse solids and suspended organic material [58–60]. There are two main configurations: gravity DMF and pressure DMF. Only in smaller SWRO plants the construction of pressure vessels turns out economically interesting. Medium to large-scale SWRO plants typically rely upon gravity DMF, providing a head on top of the filter high enough to force the seawater downward through the filtration material. Most common is a bottom layer of finer sand and a top layer of coarser anthracite. DMF units are backwashed to remove the retained contaminants in the filter material. This is performed to avoid a too high pressure drop building up over the filter. Backwash frequencies are reported to range from 7h to 48h of normal operation [60, 61]. During backwash, a fraction of the filtered water is sent back but in opposite

Table 2.2:
Overview of the main pretreatment steps in large scale SWRO plants worldwide. The capacity corresponds with the amount of fresh water produced, not taken in. A checked box corresponds with a mentioning of the process in the source(s). Abbreviations: S = Seawater, B = Brackish Water, C+F = coagulation and flocculation, DMF = dual media filtration (anthracite-sand), MF = microfiltration.

Location	Country	Capacity [m^3/d]	Feed	C+F	DMF	MF	UF	Source
Sorek	Israel	624 000	S	☑	☑	☑	□	[49]
Ashkelon	Israel	330 000	S	☑	☑	☑	□	[43]
Tuas	Singapore	318 000	S	□	□	□	☑	[50]
Al Dur	Bahrain	218 000	S	☑	☑	☑	□	[51]
Carlsbad	USA	204 000	S	□	☑	☑	□	[52]
Beni Saf	Algeria	200 000	S	□	☑	☑	□	[53]
Mostaganem	Algeria	200 000	S	□	☑	☑	□	[53]
Bahía de Palma	Spain	151 000	S	☑	☑	☑	□	[54]
Cape Coral	USA	114 000	B	□	□	☑	□	[55]
Pembroke	Malta	54 000	S	□	□	☑	□	[56]
Jeddah	Saudi Arabia	50 000	S	☑	☑	☑	□	[57]

direction (bottom-to-top). The backwash volume ranges typically from 2% to 5%, leading to a recovery of 95-98% for DMF [60]. The (micro)filtration step afterwards is to further remove the fine fraction of suspended solids and organic matter before sending the water to the RO membrane units [58–61]. The reported pore sizes for MF in the SWRO plants in Table 2.2 range from 1 to 10 μm.

In what follows, the pretreatment in the SWRO plant of Ashkelon, Israel, is shortly described as an example installation in order to provide an overview of the most interesting steps in the system in terms of MP removal (Figure 2.3). The plant has a production capacity of about 330 000 m^3/d of drinking water and is designed to provide drinking water for cities in its vicinity. This makes the Ashkelon installation one of the largest in the world. Seawater is taken in by 5 pumps (PE pipeline of 1 km) supplying in total about 840 000 m^3/d of seawater [43] that will be treated. Then, the intake water is pretreated by means of added chemicals such as NaOCl (disinfection), H_2S0_4 (pH adjustment) and $FeCl_3$ (coagulant). The first filtration step is the DMF (quartz sand and anthracite media [43]). A second filtration step is carried out by MF ("Micronic filters" in Figure 2.3). Here, the DMF typically removes suspended solids down to 10 μm [62] and potentially acts as a first significant barrier for MP in the treated seawater. The pore size of MF membranes ranges from 0.1 μm to 5 μm [63] and these membranes act as a second potential barrier for MP, given the lower size

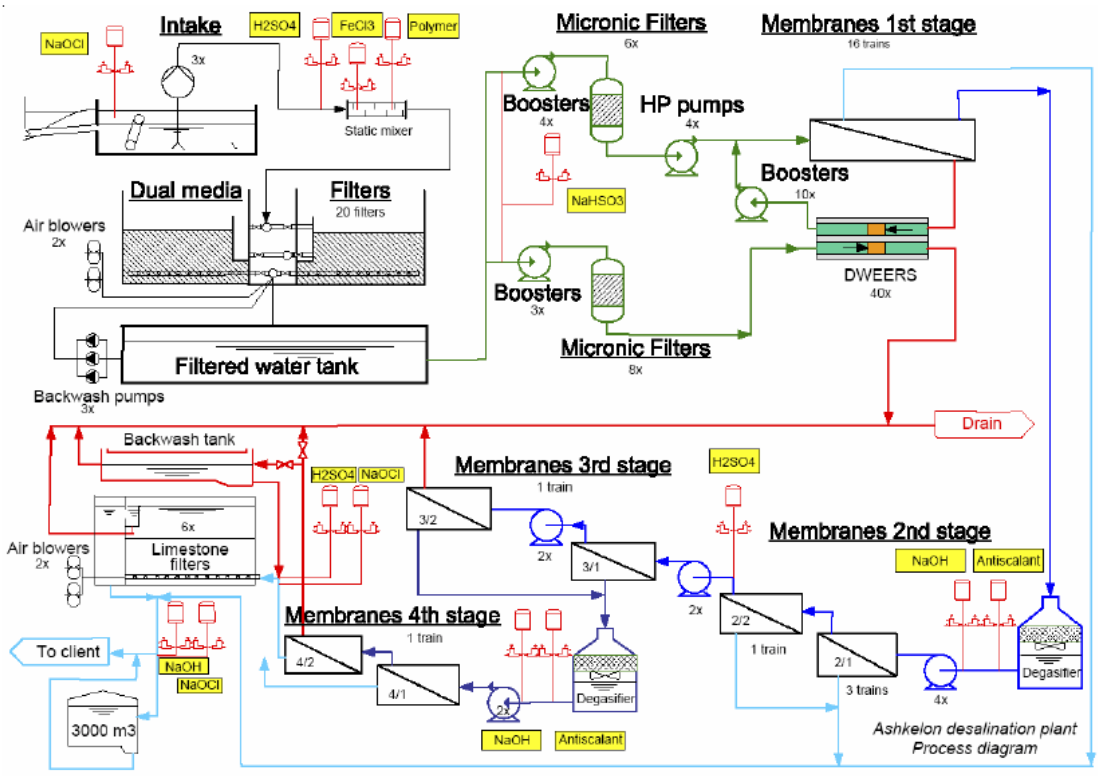

Figure 2.3: *This is a schematic overview of the SWRO plant of Ashkelon, Israel. Included are the dual media fitlration and microfiltration (Micronic filters) pretreatment steps, which form part of a conventional SWRO pretreatment. Figure from Sauvet-Goichon (2007) [43].*

limit of MP of 1 μm. Therefore, it is hypothesised that the majority of MP present in seawater are held up at least at the MF step in the pretreatment process of RO and, as a result, does not end up at the RO membranes themselves as the MP particles are by definition too big.

Previous studies that follow up the fate of MP in wastewater treatment plants (WWTP) already pointed in the direction of these unit processes as being most effective to retain MP. These studies [64–68] sample at different locations in the plant and quantify the removal of MP over every step. In Michielssen et al. (2016) for example, 3 WWTP are sampled with different treatment steps. In the end, the removal efficiency of each sampled step is reported and among the highest removal rates were a granular sand filter step and an (MF) membrane process (pore size 0.2 μm), respectively 72.1% and 99.1% [64]. In another recent study on the fate of MP in WWTP systems, a bench-scale gravity filter (anthracite-sand-gravel), typical as tertiary treatment in WWTP, is constructed to evaluate the removal of spiked MP in a WWTP slurry stream (5 mg MP/L). The authors report no breakthrough and a retrieval of more than 95% of the spiked MP in the backwash (water and air sparging, 15 min) after pouring 2L of spiked influent [68].

2.2.4 Other aspects of SWRO

Two other relevant aspects of an RO installation are the intake depth and the production of brine. The intake system is a key component of the process as it determines the feed water quality and the performance of the treatment steps down the line. The current method of choice is open ocean intake [69], as it requires lower pumping power but may lead to fairly highly contaminated water in terms of turbidity and suspended debris [70], which may include MP particles of a relatively low density. The intake depth for open water intake usually ranges from 1 to 6 m [70], with 4 m being an often encountered value [69, 71, 72]. Another option is deep intake, with pumping depths down to 35 m where the debris load is lower [69, 70]. However, this is less feasible to construct and operate and it is not used widely.

The production of brine is one of the main challenges in SWRO. It is the reject stream from the RO units and is a concentrated salt stream of high flow rate. The production of this concentrated brine is illustrated in Figure 2.4. If the salt concentration (X) is 35 g/L, and 50% of the incoming flow is eventually filtered to pure water, then half of the incoming flow will contain all salts (100% removal, in reality these values are 95% or even up to 99%). In this way, a concentrated waste stream of salt water is created (70 g/L in this example) with a flow rate that is equal to the pure water stream. This waste stream is challenging due to the environmental concerns related to its

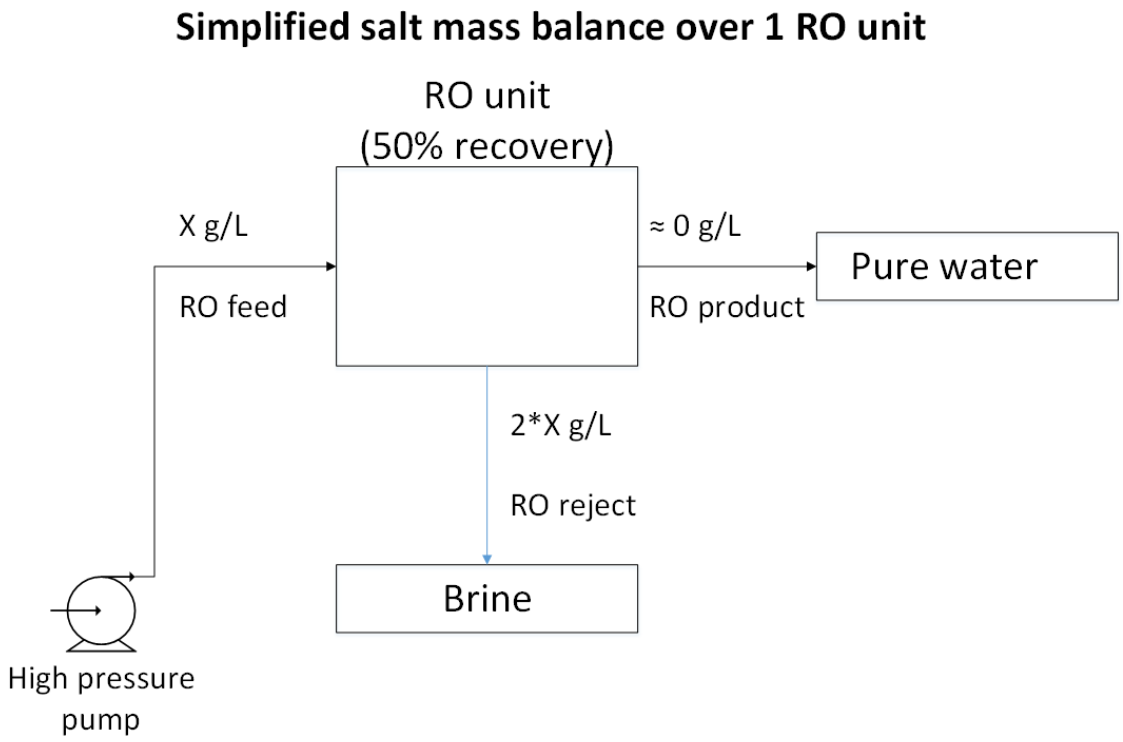

Figure 2.4: *This graphic presents a simplified diagram of 1 RO unit where X is the salt concentration in g/L. A recovery of 50% and a salt removal efficiency of 100% is assumed. This results in a concentrated waste stream of salt water (brine) with a flow rate equal to the pure water stream, i.e. half of the incoming feed to the RO unit.*

disposal in the marine environment, e.g. local brine plumes of high concentration, affecting the surrounding ecosystem. Reduced dissolved oxygen concentration, the disruption of the salt excretion system of fish and the disruption of larval development are documented ecological impacts [73]. Other concerns are the higher temperature of the brine stream and its increased alkalinity [73]. However, direct discharge back into the sea is one of the current methods to handle this waste stream with a high salt content [48]. Therefore, as it is a main environmental challenge, multiple efforts haven been taken to tackle this problem instead of direct discharge. Examples of such solutions are dilution [74] or salt recovery from the waste stream [75].

These two aspects (intake depth and brine waste) are important parameters when considering the potential removal of MP from seawater that is treated in SWRO facilities. The intake depth might influence the amount and the types of polymer taken in by the system, corresponding with the vertical distribution of MP in the water. The brine is a challenge in SWRO operation and its increased salt content (and its increased density as a result) might prove a possible resource when looking into separation of MP from pretreatment filtrates by ways of density differences.

2.3 Research Gaps

In the following research, the main goal is to look into the possibility of removing MP particles taken in by SWRO installations. However, there are still many gaps in the literature about the behaviour of the MP. First of all there is the occurrence issue. By now there have been various sampling studies to identify and quantify the presence of MP pollution in the oceans and seas. Yet, there are limits to these findings such as the lower size limit of sampled particles or the depth at which samples are taken. Up to now, the smallest fraction of MP (< 50 μm) is barely included in measurements and there is little known on the occurrence and distribution of the MP deeper in the water column, the so-called 'lost' plastics (Section 2.1.2). These issues give rise to the incomplete image there is concerning the marine MP pollution.

Secondly, how do MP behave in the natural environment of ocean and seas? Wind, waves and currents are forces that act on the particles while degradation and bio-fouling influence their characteristics, such as shape, size and density (Section 2.1.3). These factors influence the vertical distribution and at the same time the fraction that might be taken in by SWRO pumps.

Thirdly, how do MP behave throughout the process of SWRO? The MP present in the seawater taken in by SWRO plants pass the same process steps as the water. For this reason, it will be interesting to investigate their behaviour and the removal efficiency of these various steps in order to point out where the hotspots of MP occur within the process. Earlier studies already point to the strong removal capacity of unit processes such as gravity filters and MF membranes in terms of MP in WWTP. However, the previous bench-scale study on DMF focussed on WWTP streams and only filtered a 2L spike, not allowing a longer operation with a more continuous spike which may influence the result of MP retrieval in the backwash stream [68]. If the long-term operation and MP removal of this step in the context of SWRO is further investigated, this will allow to act more effectively in terms of the removal of MP from the reject streams created in DMF and MF before these streams would end up back into the seawater, including the MP particles. In the following chapter, the main research questions of this thesis are formulated to answer some of these research issues.

CHAPTER 3

RESEARCH OUTLINE

3.1 Research Questions

MP pollution is a growing threat for marine ecosystems and as a pollutant, the particles act as a hazard in multiple ways. It is clear from the above that research concerning this MP pollution is very hard to characterise and to generalise. There are many factors to be taken into account: vicinity of pollution sources (e.g. industry, cities or fishery), ocean currents, wind conditions, polymer type and density, rate of biofouling, etc. Therefore, it is hard to quantify the presence of these MP particles in the seawater. However, their presence has been evidenced and their impact as well. Therefore, this research will focus on a method to remove a fraction of the MP present in seawater relatively close to coastal areas, where concentrations are typically higher than in open water (2.1.2). SWRO installations draw in big flows of seawater to produce e.g. drinking water. This implies that the MP contained in this seawater also pass through the system and, as it they are not known to be removed or processed, end up in the sea again as part of the pretreatment reject streams.

In this view, this research will firstly focus on the behaviour of MP in seawater and how biofouling phenomena influence its density. This will give an indication of the behaviour of MP in the vertical water column, rather than only at the surface of the water. It is assumed that, due to biofouling, the less dense polymers (PP and PE) will sink, but much slower than for example PVC or PET particles. The aim of this set-up is to evidence the probability of taking in predominantly PE and PP particles when pumping at rather shallow depths, as happens in SWRO installations 2.2.4.

Secondly, as can be seen in Table 2.2, many large-scale SWRO plants incorporate both DMF and MF as a pretreatment of the incoming water before it is sent over the RO membranes. Therefore, there will be an attempt to describe the behaviour of MP throughout these pretreatment steps common in SWRO installations and how efficiently this pretreatment functions in terms of MP removal. Also, the quantification of the MP contained in the resulting streams poses a big challenge and the way

these problems are answered during the analysis of the results will also feature as an important aspect of this research study.

Finally there will be an attempt to construct a mass balance to estimate the flux and distribution of MP particles present in the seawater treated in SWRO installations. This allows to create a more specific image of the presence and fate of MP in these installations and to discuss their potential for removal from the process streams.

3.2 Experimental Research

In order to answer these research questions, both predictive calculations as well as experimental research will be conducted. The experimental part of this research is mainly designed to study the behaviour and fate of MP particles in SWRO installations. On the one hand, more information about the effect of biofouling on the floating behaviour of plastics in seawater is relevant to better predict what kind and how many MP enter an SWRO treatment process. On the other hand, removal efficiencies of MP in the different subprocesses within the SWRO system are necessary to describe the flux of MP and to make predictions concerning removal and recovery potential of (micro)plastics.

As described in 2.1.3, earlier experimental work supports the hypothesis that **biofouling** influences the density and floating behaviour of MP. To further comprehend this phenomenon a first experimental set-up is designed to study the influence of biofouling on the density of plastic particles. More specific, the goal of the experiment is to quantify the increase of density in relation to the amount of biomass present on a certain particle.

Later on, a bench-scale simulation of **SWRO pretreatment processes** is constructed and evaluated in terms of MP removal. The goal of the experiments is to predict where the MP will end up during the passage through a series of pretreatment steps for RO.

Finally, on the one hand, an estimate of the **plastic flux** throughout large-scale SWRO installations will be performed based on data retrieved from literature. On the other hand, based on the experimental results from the bench-scale pretreatment simulations, a **mass balance** over both unit processes (i.e. DMF and MF) will be constructed to further elaborate on the flux of MP in SWRO installations and on their potential for removal.

CHAPTER 4

MATERIALS AND METHODS

4.1 Biofouling

4.1.1 Tank Set-up

Highly-spherical plastic particles of the two polymer types of highest interest, namely PP and PE, are used in this experiment on biofouling. The virgin PP spheres have a density of 0.90 g/cm^3, are more than 95% spherical, are white and have a diameter of 2.45 ± 0.05 mm (Cospheric, USA). The virgin PE spheres have a density of 0.98 g/cm^3, are more than 90% spherical, are red and more than 90% of the particles have a

Figure 4.1: *The 4 different kinds of MP that are used during the experimental phase of this research: white PP (2.45 ± 0.05 mm, top-left), red PE (600-710 µm, top-right), green PE (90-106 µm, bottom-left) and white PE (10-45 µm, bottom-right) (Cospheric, USA).*

diameter between 600 μm and 710 μm (Cospheric, USA). As the shape and size of the polymer spheres are very uniform, the variation in density can be attributed to the amount of biofouling that occurred during the experiment.

In a first experiment (Biofouling 1, Figure 4.2a), the polymer beads are suspended in natural seawater (North Sea, Belgium) in a tank (60x30x35 cm^3) by means of a cage, which is sealed at both ends with a 500 μm membrane. In this way, the beads stay in the seawater while water, nutrients, oxygen and microorganisms can pass through the cage, in order to allow biofouling to take place. One aeration tube is provided and the set-up is located in a controlled temperature room (15 °C). As described in 2.1.3, biofouling is observed within days and continues to increase within the first weeks. Samples of the fouled beads are taken after 0, 1, 2, 4 and 6 weeks and are used for density measurement and ATP (adenosine triphosphate) measurement.

In a second experiment (Biofouling 2, Figure 4.2b), the conditions for the biofouling are altered. The tank with natural seawater (North Sea, Belgium) is placed in another controlled temperature room (25 °C). Also, marine sludge, which is collected at the moment of start-up, is added to the tank. Like this, the amount of biological active mass present in the tank is higher at the start of the experiment. Both alterations aim to promote the growth of marine biomass in the tank. The marine sludge is scraped off of wooden pillars (Figure 4.3a) and concrete blocks (Figure 4.3b), all found on the North Sea coast of Breskens and Cadzand. Due to practical limitations, for this second run only the smaller PE beads are studied. The other conditions and sample methods are the same as in the set-up of Biofouling 1.

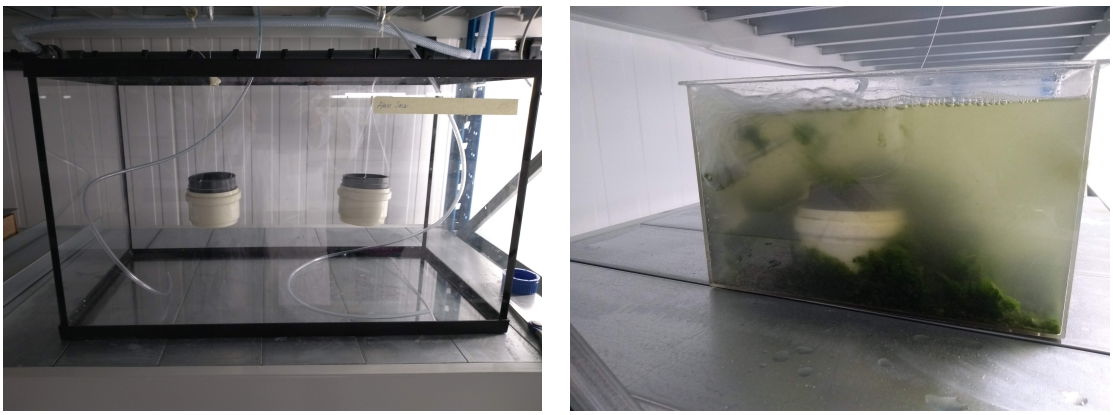

(a) *Set-up for Biofouling 1 (15 °C)* ***(b)*** *Set-up for Biofouling 2 (25 °C)*

Figure 4.2: *The two tanks for both biofouling experiments, with altered conditions: difference in room temperature and addition of marine sludge.*

(a) *Wooden pillars (Breskens)* ***(b)*** *Concrete blocks (Cadzand)*

Figure 4.3: *Locations of the marine sludge added to the seawater tank for the biofouling experiments.*

4.1.2 Density Measurements

The goal of these set-ups is to study the influence of the presence of biofouling on the MP density. From every week's sample, 10 PP beads and 80 PE beads are carefully transferred from the cages to a beaker containing demineralised water for density measurement. The experiments as described here are performed immediately after collection to avoid breakdown of the biofilm formed on the beads. To measure the density, the beads are initially placed in a beaker containing demineralised water with a measured density of 0.99 g/cm^3 (at 20°C). The beads stay afloat and then ethanol (indicated density: 0.79 g/cm^3) is added by means of a glass pipette to decrease the mixture's density. Whenever beads start to sink, the density of these beads is assumed to be equal or above that of the liquid. At this point, the mixture's density is measured using a DMA 5000 density meter (Anton Paar, Austria).

The procedure is repeated 2 times for every week's sample, each time with 5 or 40 beads per beaker, respectively, for the PP and PE beads. During every repetition, ethanol, milliQ water and demineralised water, which is used to prepare the ethanol-water mixture, are also measured with the DMA 5000 to follow up the performance of the density measurement. For the samples, the mixture is always injected thrice into the capillary tube of the DMA 5000 and an average value is calculated for every sample. The DMA 5000's measuring temperature is always set at 20.00°C for reproducible results.

4.1.3 ATP Measurement

On the same day of the density measurement, another sample was taken of 30 PP beads and 500 PE beads, by means of visual counting and a clicker to keep count.

The beads are then carefully placed in a beaker of 10 mL of milliQ water. A sonication procedure (15 minutes at 30 °C) is performed to remove all biomass present on the beads and transfer it to the water phase. These conditions are selected to be long enough to allow the removal of biofilm from the plastic particles, while keeping the temperature at the lower limit of the machine to minimise a temperature shock effect for the microorganisms. This water phase is then analysed for ATP concentration with a luminescence measurement using an Infinite 200 PRO Series Multimode Reader apparatus (Tecan Trading AG, USA). After addition of BacTiter-Glo^{TM} (Promega, USA), the luminescence intensity is measured which is related to the ATP concentration in the samples. The relation between the signal and the ATP concentration is followed up by adding a dilution series from a reference sample of ATP in a 96-well tray (Greiner Flat Black, Greiner, Austria). During the Biofouling 1 experiment, the tray is filled with 2x30 volumes of 100 μL from the sonicated samples of either PE or PP (total of 60). During the Biofouling 2 experiment, as there were only PE beads, the tray is filled with 1x60 volumes of 100 μL from the sonicated sample of PE beads.

4.2 SWRO Pretreatment Simulation

4.2.1 Dual Media Filtration

The main set-up during this research is the dual media filter (DMF) that consists of anthracite and sand. As mentioned above (Table 2.2), this type of DMF is very common as a pretreatment step in the larger SWRO plants. The bench-scale filter was constructed using a hard PVC pipe (1 meter in length and an internal diameter of 34 mm) which is sealed at both ends using a wire gauze of mesh size 60 to keep the filter material in place during running and during backwash operation. The mesh retains the sand and anthracite particles but is large enough for the studied MP material and water to pass freely. In this way, the gauze does not add to the filtering effect of the DMF itself. The coarse upper layer of the DMF consists of anthracite (size range: 1 to 2 mm), the finer lower layer consists of sand (size range: 0.250 to 1 mm). Before the implementation, both materials are dried in an oven overnight at 50 °C and sieved in different fractions from which the preferred size fraction is retained. After filling the column with the filter material, it is first conditioned during two days with unspiked water to rinse the remaining smaller sand and anthracite particles (< 250 μm) out of the column in order to ensure a clean operation and to avoid fast clogging of the filter papers on which the MP are eventually collected. After this procedure, the column is ready to operate and treat samples of tap water and seawater spiked with MP.

During this experiment, the column is in operation for a total of 4 weeks. In a first phase, tap water is used as the matrix to evaluate the performance of the column in terms of removal op MP. The samples are prepared in the following way: 30.0 mg of green PE beads (90-106 μm, Cospheric, USA) are weighed and treated with a 0.1 %(v/v) Tween 80 solution. Tween has an emulsifying effect and reduces the hydrophobicity of the virgin beads, as recommended by the producer. Then, the 30 mg green PE is added to 10L bottles of water. The exact amount of spiked PE in terms of number of particle is of course unknown in this way, which is countered by executing and analysing empty column runs as described below. In a second phase, seawater is used, spiked with the same MP particles as in the first phase, but in a concentration that tends to approximate more realistic values. In this case, 3 mg of PE beads is added to the 10L bottles of seawater. In the second phase (with seawater), smaller white PE beads (diameter: 10-45 μm, (Cospheric, USA)) are also added at 3 mg per 10L bottle in addition to the 3 mg per 10L of green PE beads (diameter: 90-106 μm).

The influent feed is constantly stirred by a magnetic stirrer on the bottom of the bottle to homogenise the MP concentration in the feed while it is being pumped over the filter column. All connections for water flows are constructed using Festo (Germany) norprene tubes and fittings. A Masterflex L/S-Economic Drive pump 115 VAC (Cole-Parmer, USA) is installed which was used for both normal (top-to-bottom) and backwash (bottom-to-top) operation. Switching between both regimes is possible by swapping the tubes of the installation. The pump is able to operate between 0.072 and 174 L/h and it is calibrated before each filtration period at 9 L/h for normal operation. This corresponds with a loading of 10 $m^3/m^2/h$ on the used column which is a typical value for DMF. For backwash, the pump is set to a flow of about 36 L/h [61]. This way, the backwash is performed with a flow rate 4 times higher than the normal operation, flushing the column with 6L of fresh water during 10 minutes. This leads to a recovery of 94% (6L of the total of 100L filtered water is used again for backwash) for this bench-scale system. During backwash, the filter material is allowed to fully expand, taking up almost the entire volume of the column (1m height) while the built up contaminants, including the spiked MP, are loosened from the anthracite and sand and are flushed out by the upstream water flow. After backwash, the filter material settles gradually with the heavier sand settling at the bottom again. The lighter anthracite settles on top of the sand, allowing a new run of normal operation. More design parameters are listed in Table 4.1. Figure 4.4 provides a sketch of the DMF set-up.

Both effluent and backwash water are collected for analysis on MP content. The resulting streams are immediately passed over a round white Grade 2 filter paper (Whatman, USA) for collection. The filter paper's maximum pore size is 8 μm. In this way,

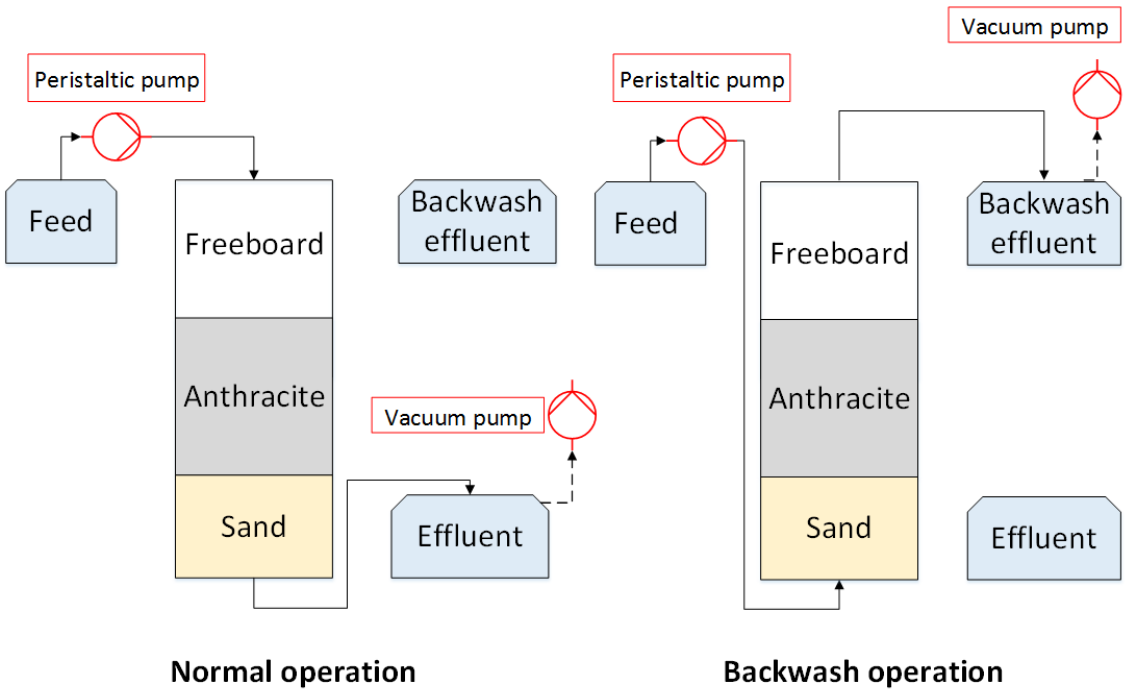

Figure 4.4: *This sketch represents the bench-scale set-up for DMF filtration. The feed is spiked with MP and sent over the filter material in the column (normal operation, top-to-bottom). During backwash operation, the connections are changed so a fraction of the filtered water can be sent back through the filter material for cleaning (bottom-to-top). The vacuum pump is installed to allow direct collection of the effluent or the backwash stream on paper filters.*

all matter including the spiked MP (which are bigger than 8 μm) are concentrated, which allows faster analysis of the MP by means of microscopy (cfr. Section 4.2.4).

Finally, in addition to the quantification of MP concentration of influent, effluent and backwash streams, the vertical progress of the spiked MP beads throughout the filter media of the column is followed up. During operation, this is performed by visually inspecting the filter material after every 10L treated (i.e. about every 1 hour and 5 minutes at a speed of about 9 L/h) and locating the deepest MP that is discernible with the naked eye. Then its depth is measured, being the positive distance measuring downwards starting from the top of the filter material itself. Of course, this can only be considered as an indicative value of the vertical progress of the MP. The individual beads may be invisible to the naked eye or are simply missed by the observer or they could be present in the core of the column rather than on the outside.

Therefore, at the end of both phases (i.e. each time after 10 days of operation), the final fifth backwash is not performed and rather, the filter material is removed systematically from the column. The bed is divided into 10 zones of 6.7 cm and these solid samples are put in an erlenmeyer flask, which is then filled up to 400 mL with demineralised water. The erlenmeyers are thoroughly shaken to release all MP present in the sampled filter material (anthracite and/or sand) at 200 rotations per minute during 1 hour. Then, they are allowed to settle with the lighter MP of 0.98 g/cm^3 floating

Table 4.1:
Overview of the design parameters of the bench-scale DMF (anthracite-sand) with corresponding values encountered in theoretical literature and/or actual operating conditions.

Parameter	Value	Unit	Literature	Source
Column characteristics				
Diameter	0.034	m	–	–
Total Height	1	m	–	–
Anthracite (bed height L_1)	0.40	m	[0.30 - 0.60]	[61]
Sand (bed height L_2)	0.27	m	[0.15-0.40]	[61]
Anthracite/sand ratio	1.5	[−]	1.5	[61]
Dual Filter (bed height)	0.67	m	[0.45-1]	[61]
Freeboard (height)	0.33	m	–	–
ϵ (m freeboard/m total bed)	0.5	[−]	>20%	[61]
Anthracite Effective Size ($d_{p,1}$)	≈ 0.91	mm	–	[76]
Sand Effective Size ($d_{p,2}$)	≈ 0.45	mm	–	[76]
$\Sigma(L_i/d_{p,i})$	1032	m/m	[1000-1500]	[60]
Operational characteristics				
Loading rate	10	$m^3/m^2/h$	[8-12]	[61, 77]
Flow rate v	9	L/h	8	[43]
Backwash flow rate	36	L/h	$[3\text{-}5] * v$	[61]
Backwash frequency	0.46	d	[0.29-3]	[43, 60, 61, 77]
Backwash duration	10	min	[3-10]	[61]

on top of the water and the filter material settling on the bottom. The resulting mixture is poured over a double filtration system with the 60 mesh wire gauze (the same gauze that is used before to keep the filter material in place in the column itself) followed by the grade 2 filter paper in order to concentrate the MP that were present in the solid samples. Eventually, the isolated MP are also analysed by microscopy. In this way, the progress of MP throughout the filter material can be quantified in a more reproducible manner by the number of MP present in all 10 zones.

During the total of 4 weeks, the DMF was in operation with a daily treatment of 50L of spiked water (tap water or seawater). This gives rise to runs of 100L between every backwash of 6L (= 6% of the total effluent is used again for backwash). In other words, an operational time of little over 11h (100L/9(L/h)=11,11h). Every run results in 10 collection filter papers for effluent (refreshed every 10L) and 6 for backwash (refreshed every 1L). For both the spiked tap water and the spiked seawater, 5 runs (5x2 days) are executed. Additionally, empty column runs are executed to be able to describe with higher certainty the outcome of the experiments in terms of removal efficiency. The empty column runs are run through an empty column (i.e. without filter material) with the same spiked water and they are also collected and analysed on the same filter papers (Grade 2, Whatman). On the one side, this allows to estimate the amount of MP that enters the system initially with either the 3 mg/L or 0.3 mg MP/L spike and, on the other side, these empty runs account for the losses that occur throughout the system such as stickiness of the tubing or dead zones in the column or the fittings.

In the second phase of this DMF set-up (all the runs with seawater in Table 4.3), it was mentioned that smaller PE beads (white, 10-45 μm, bottom-right on Figure 4.1) are also added as a spike to the influent water. In the first place, it was intended to check whether it was possible to follow their vertical progress qualitatively through the filter material, just like was done for the green beads. However, it turned out impossible to visually discern any of these beads in the column. For that reason, it was chosen to pass a small fraction of the total volume (2x1L of every run's 100) over black filter paper (Grade 918, 90mm diameter, Camlab Ltd) instead for a qualitative study of the possible breakthrough of these smaller beads in the effluent of the DMF column. This is an interesting addition to the experimental set-up as these MP represent the lower limit of the MP size range, which are of major importance in research on MP in general.

4.2.2 Microfiltration

Using a similar set-up as for the DMF experiment, this study was also performed for the microfiltration (MF) pretreatment step which usually follows the DMF step in the SWRO pretreatment process (Table 2.2). Given the available PE MP to spike influent samples (90-106 μm), an MF cartridge of 25 μm (Van Marcke Pro Purifo, Belgium) was installed. This MF cartridge has a height of 315 mm and a diameter of 135 mm, resulting in a filter surface area of 0.134 m^2. The filter works according to the outside-in principle: water surrounds the outside of the MF filter and is forced inwards, from where the water can leave the filter cartridge at the top. In practice, MF membranes are also backwashed frequently to ensure proper operation and to counter the transmembrane pressure that builds up due to fouling of the membranes. This backwash is also simulated during the experiment in order to follow up the fate of the MP, similar to the DMF experiments. For every experiment, there is also an empty run during which the MF cartridge is uncoupled and 1 run of 6x10L with spiked influent is passed through the system. Again, the reason for this empty run is to counter the loss of MP in the tubings, fittings and cartridge holder and to be able to quantify more accurately the amount of MP that actually passes the system and to construct a total MP mass balance in the end.

Each experiment consists of 60L of pretreatment after which the MF module is backwashed to remove the built-up contaminants from the MF membrane. Backwashing is only performed at the end of each experiment as long as there is no significant decrease of filtration speed during the experiment. The feed water (tap water or filtered seawater) do not give rise to quick membrane fouling that decreases the filtration speed. This is the reason the duration of 1 MF run is higher than what is typically

Table 4.2:
Overview of the design parameters of the bench-scale MF cartridge filter with corresponding values encountered in theoretical literature and/or actual operating conditions.

Parameter	Value	Unit	Literature	Source
Column characteristics				
Diameter	0.135	m	–	–
Total Height	0.315	m	–	–
Filter Surface Area	0.134	m^2	0.1	[57]
Operational characteristics				
Flow rate *v*	9	L/h	[8-24]	[57]
Backwash flow rate	36	L/h	[31-40]	[57]
Backwash frequency	6.7	h	[0.5-1.5]	[57]
Backwash duration	6	min	[0.67-2]	[57]

found in MF experiments. The MF membrane module characteristics and operational parameters are all listed in Table 4.2.

This MF procedure is executed once with tap water and once with filtered seawater and both with different spikes of MP beads. Both experiments are performed in parallel with both DMF experiments, feeding the MF module with the same concentrations of green MP (respectively 3 and 0.3 mg MP/L). Before preparing the feed water, the MP are again treated with a 0.1 v/v% Tween solution. Influent, effluent and backwash water were passed over the same filters as in Section 4.2.1. In parallel with the DMF experiments, the smallest white MP have also been added (0.3 mg MP/L) with the goal to qualitatively investigate the possible breakthrough of these smaller particles, as compared to the larger green MP. For this, 2x1L are also filtered over a black filter to follow up their fate during the experiment. An overview of the entire experimental schedule, for both the DMF and the MF experiments, is also given in Table 4.3.

Table 4.3:
Conditions of the different experiments to simulate the pretreatment of SWRO and to evaluate their removal efficiency of MP particles.

Operation	Code	Duration (days/run)	Runs	Concentration (mg MP/L)	Volume (L/run)
Dual Media Filtration					
Spiked tap water	DMF1	2	5	3	100
Spiked seawater	DMF2	2	5	0.3	100
Microfiltration					
Spiked tap water	MF1	1	1	3	60
Spiked seawater	MF2	1	1	0.3	60

4.2.3 Contamination and Storage

No blanks were kept in terms of contamination from the air, clothing or other sources of external MP during operation of both the DMF and MF experiments. The results of all experiments depend on the counting of the spiked MP beads of known size and

colour. These spikes are always of a high concentration and it is further assumed that the contamination by external particles (plastic or other) of the same size and colour is negligible.

The spatulas to place and remove the filter paper and the Buchner filter holder itself are rinsed with demineralised water during every replacement of a filter paper. All resulting filters are stored in fitting Petri dishes (90 mm) to prevent the loss of filtered MP beads between collection and microscopic analysis. During the microscopy analysis, blue nitrile gloves are worn to handle the filters. The glass surface of the microscope is rinsed between every filter to prevent contamination of the spiked MP beads between filters.

4.2.4 Microscopy Analysis

In the end, the performance of both the DMF and the MF set-up is followed up by means of filtering the effluent and backwash streams, concentrating the spiked MP on paper filters. Eventually, these filters are analysed by means of pictures taken by a camera connected to a microscope and analysed through imaging software. The resulting filters are analysed in two different ways, depending on a first visual inspection of the filter. If none or barely any green MP are visually detectable, which is typical for the effluent filters, the MP are counted individually by scanning the entire filter with the microscope (Olympus SZX10 Stereo Microscope) and counting the plastic spheres present one by one. This gives an exact number of MP present on a filter.

If filters (influent and backwash filters) contain many more particles after visual inspection, it is chosen to take microscopic pictures of the filter and further analyse these with an imaging software to quantify the results. The reason for this alternative method lies in the fact that the amount of MP is too high to count individually in these cases.

4.2.5 Quantification and Counting Method

During this second part of the experimental research, the quantification of the results arises as a major challenge. Therefore, some additional analyses and tests are performed to accurately quantify the results of the experiments. First of all, when preparing the spiked feed water, the standardised MP are weighed down to an accuracy of 1 mg. However, the resulting paper filters that contain the MP from the different streams no longer allow weighing the plastics because it is possible that other particles are present as well, especially on the backwash filters. Also, the accuracy would be very low to compare the different outcomes. In the end, as mentioned

above, the MP are counted or estimated number-wise and a series of measurement and calibration steps are performed to eventually establish a method that allows the quantification of well-defined MP (in this study green, spherical particles with a diameter around 100 μm) on a certain filter with a reliable degree of certainty. This calibration consists of 3 different analyses (cfr. Table 4.4).

Table 4.4:
Overview of the series of calibration steps performed to allow a relation between mass of MP and the number of MP eventually present on a collection filter paper from the experimental work. In the end, it is necessary to be able to relate the measured pixels with the expected number of MP on the filter.

Calibration	Relation	Method
1	Mass-Expected Number	Mastersizer: d_{50}
2	Pixel-Counted Number	ImageJ: 20 sample pictures
3	Counted Number-Expected Number	ImageJ: standard series

1. Mass-Number Relation

First of all, as the spikes are prepared based on the mass of the MP and the results are expressed as the amount of individual particles, a relation between mass and number is required. In order to obtain this relation, the green PE particles are analysed using a Mastersizer 2000 (Melvern Panalytical, UK) to accurately determine a particle size distribution (PSD) and an average diameter d_{50} which can be used to relate the mass to a number of particles.

The size analysis is based on laser beam diffraction caused by the analysed particles. A polydisperse distribution is used during the analysis so a dust fraction that might be present in the product can also be detected. The size range of the machine is 0.02 to 2000 μm. Eventually, the final result can be determined in 2 ways by the Mastersizer, either according to the Mie theory or the Fraunhofer theory. After comparison of the results using both methods, it is chosen to further use the Mie theory as the results for the MP size range (around 100 μm) are similar while the Mie theory is more accurate for particles < 25 μm, which is interesting to better detect a possible dust fraction. The MP for analysis are again first treated in a 0.1 v/v% Tween 80 solution in demineralised water, for the same reason as described earlier in Section 4.2.1. This is necessary to avoid aggregation of multiple particles, which would give rise to various peaks during the particle size measurement.

The measured MP are lighter than the liquid in which they are sent through the Mastersizer and the inlet is at the bottom. This problem is countered by adding a mixing rod to the inlet compartment. However, too powerful mixing may give rise to air bubbles in the feed liquid which also diffract the laser beam. This phenomenon influences

the measurement as the air bubbles are also measured, typically as particles smaller than the green MP size range.

The Mastersizer is typically operated in a closed system set-up, where the analysed liquid is sent back to the feed compartment and is sent through the Mastersizer. This leads to a second practical problem that is also related to the low density of the MP. The relatively smaller particles stay in suspension longer that larger ones, which leads to a bias towards smaller sizes as the smaller particles may be sent through the system more frequently than large particles. For this reason, it is chosen to operate the analysis as an open system. The analysed fraction is collected in a separate compartment and is not sent back through the system. This leads to a higher chance of air bubbles as the liquid surface gradually decreases and approaches the mixing rod. The solution for this issue consists eventually of manually adjusting the mixing rod to avoid bubble production and intermittently interrupting the analysis to allow the bubbles to escape the feed liquid. The open system also implies interrupting the system after every repetition and pouring the analysed liquid back in the feed compartment, which gives rise to air bubbles again. This is countered by allowing enough time between every analysis so bubbles can again escape the feed compartment before starting up a new analysis.

2. Pixel-Number Relation

Secondly, it is necessary to establish a method to estimate the amount of particles present on a filter when it is impossible to count them individually. In order to do this, pictures are taken by means of a microscope and the surface that belongs to green particles in terms of pixels is measured. This is possible as the camera connected to the microscope always takes pictures from the same height and with the same magnification. During this calibration, 20 random sample pictures are selected where the amount of MP is in the order of magnitude of 10 to 100. Firstly, the MP are counted visually on the picture. Then, the same picture is analysed using the imaging software ImageJ (IJ 1.46r, USA). The processing of the images is explained below, in Section 4.2.6. From this test, a relation between the average amount of pixels and the corresponding amount of MP is obtained. In other words, it is determined how many pixels 1 green MP occupies on average.

3. Evaluation of Counting Methods

Thirdly, another calibration test is designed to quantify the accuracy of a method and to eventually select the best performing method. Two counting methods are

tested because the microscopic pictures are unable to cover the entire filter. Also, the nature of the experiments leads to very heterogeneously spread patterns of MP on the resulting filters, which complicates accurate estimates of the entire amount of MP on one filter. The tested methods are: (1) 20 randomly taken pictures of known and constant surface from which an average value is extracted and extrapolated to the surface of the filer (= "Method 1"); and (2) 28 to 30 pictures of fixed parts that cover the entire filter that are processed in a way that all results can eventually be added up to estimate the total amount of MP present on the entire filter (= "Method 2"). The calibration test to evaluate the performance of both methods is based on a series of 12 filters on which very precisely weighed amounts of the green MP, that have been used throughout the experiments, are transferred. This standard series of 12 filters containing known amounts of MP is prepared and handled in the same way as the experimental results. This allows to relate the estimated amount of MP with a theoretically expected amount of MP based on the measured mass at the start so the accuracy of a method can be evaluated.

4.2.6 Data Analysis

During the biofouling experiments, the density data are analysed using Microsoft Excel and the statistical software R. The ATP data are analysed using Microsoft Excel. The results from the Mastersizer analyses, from which an average diameter (d_{50}) is extracted, are treated in Microsoft Excel. During the pretreatment simulations, the resulting filters are processed and analysed using ImageJ. The processing consists of cutting out the desired region of the picture and blurring out the noise inherent to the background of the filter paper itself using the "Smoothen" function. Then, a colour threshold was defined based on the HSB characteristics (Hue, Saturation and Brightness) of the colours of a picture, every time set at respectively [70-135], [40-255] and [0-255]. In this way, it is possible to selectively isolate the pixels of the green beads from the background. The resulting pixels are related to an amount of MP by means of the results of the performed calibrations. Further analysis of the results is performed in Microsoft Excel. All data in Chapters 5 and 6 are reported with the standard deviation.

CHAPTER 5

RESULTS

5.1 Theoretical Considerations: Microplastic Density and Water Density

Before presenting the results from the experimental work, some theoretical considerations are made in relation with the density of MP and of the reject streams in the SWRO process. MP density has been studied by following up the influence of biofouling on a particle's density (cfr. Section 5.2). The density difference between MP particles and the SWRO reject streams will also return in Section 6.2 in a series of simulation calculations concerning the SWRO process.

Table 2.1 shows polymers have different densities and they differ from the density of water. Under normal conditions, all plastic particles will either float (lower density) or sink down (higher density). In this research, density will come forward as an important parameter in the studied systems. Water density is variable and especially salt content and temperature exert an influence on this property (Figure 5.1). However, temperature's influence is much smaller than salt content's influence. This also means that the RO brine is denser than the backwash streams from the DMF and/or MF in which the MP are retained. As a result, it might be possible to alter the medium in which MP are present by mixing with the brine stream. Figure 5.2 relates the density differences between pure water, seawater and RO brine with the densities of different common polymers, as mentioned in Table 2.1. This shows that only two types (PE and PP) are well below (sea)water's density and that the brine from the example calculation (Figure 2.4) is not that much denser in the sense that it possibly only includes one more polymer type (PS). It appears that density differences of polymers are too big in relation to the increase in density of seawater after concentrating the salts during the RO process. This points in the direction that a direct application of this waste stream will not produce an added value in the search for a cost-effective removal of MP from the SWRO reject streams. This will be further discussed during the simulation calculations in Section 6.2.

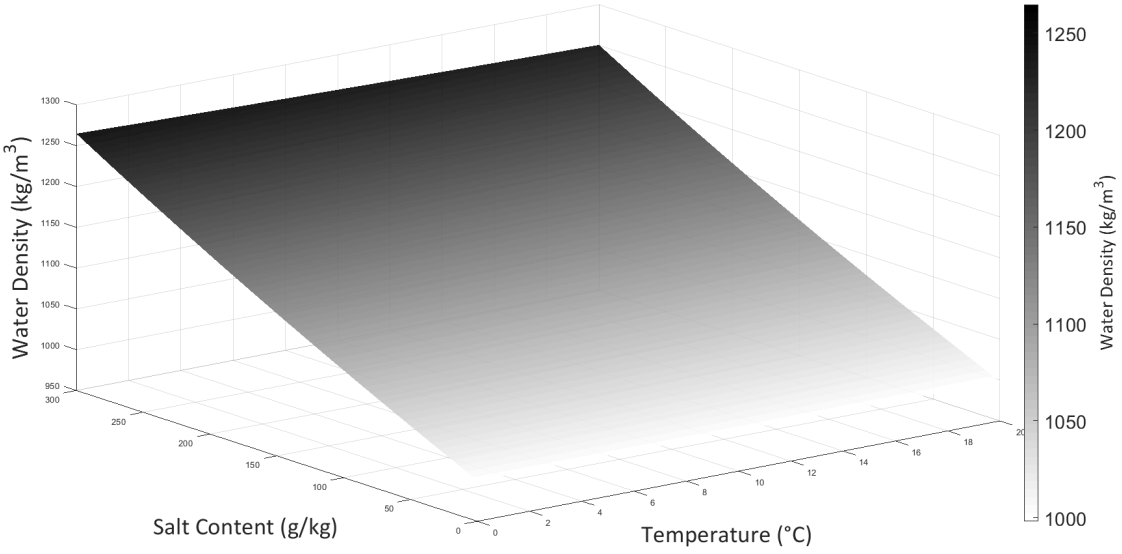

Figure 5.1: *The density of water (kg/m^3) depends on both its salt content (g salts/kg water) and on its temperature (°C). According to the model developed by Millero & Huang (2009) [78].*

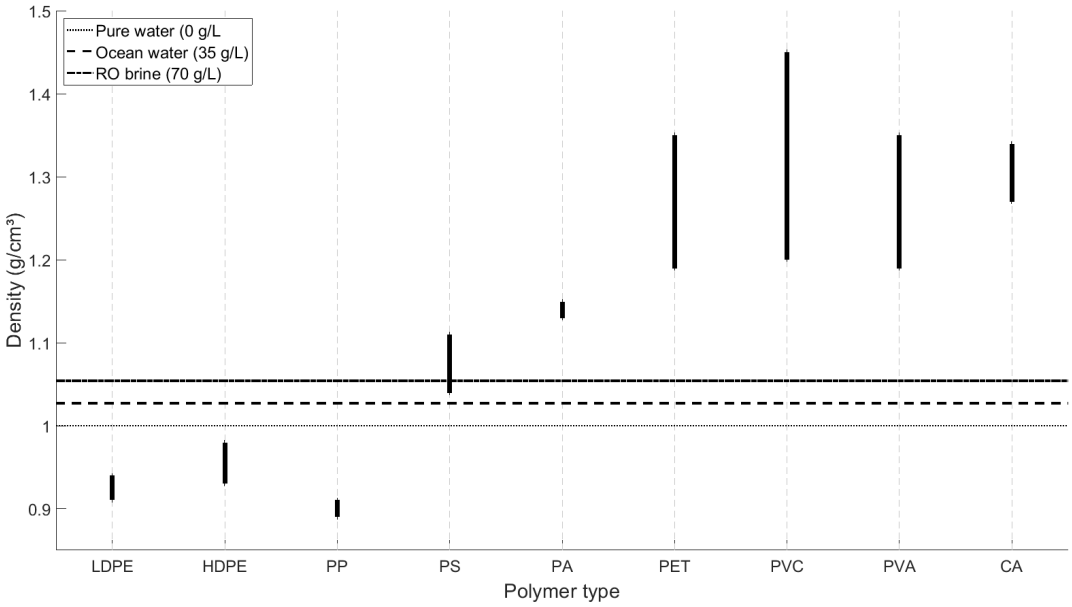

Figure 5.2: *The density ranges provided in Table 2.1 are visualised in this graphic. Also, typical densities for pure water, sea water and reverse osmosis (RO) brine are shown as a reference (density data are retrieved from Andrady (2011) [1]).*

Nevertheless, PP, LDPE and HDPE are initially positively buoyant in seawater (i.e. the density of pristine particles is lower than seawater density) and in many sampling studies they come forward as the most abundant plastics contributing to floating debris [12, 18, 19]. In modelling studies they also come forward as the most relevant polymer types with respect to the water column [17, 38]. On the one hand, this can be explained by its relatively large share of the worldwide production of plastics (cfr.

Table 2.1) which is about 62%. On the other hand, heavier polymers will rather sink down once they are released as (micro)plastic polymers and are less dependent on the fouling of their surface to increase density. As a result, when intake pumps of SWRO installations are installed in the upper layers of the ocean or sea (1 to 6m depth), it is possible that the largest fraction of MP taken in is of a relatively lower density, namely those of PP, LDPE and HDPE. This situation is also assessed in the simulation calculations in Section 6.2.

5.2 Biofouling

For the big PP beads it is possible to discern the sinking of every particle individually, in such a way that every measured sample can be related to the density of 1 plastic particle. From all measured plastic beads, an average value per set of measurements can be retained. For the PE beads, the sinking happens more continuous and not one by one. Using R, there is significant proof ($p << 0.05$ for each set) that every set of measurement can be approached by a normal distribution, from which an average density, i.e. the midpoint of the cumulative sigmoid function and the corresponding standard error, can be extracted.

Figure 5.3 shows the results of the first experiment (Biofouling 1) and Figure 5.4 those of the second experiment (Biofouling 2), as described in Section 4.1. The measured ATP concentration of the plastic particles and their corresponding density are plotted throughout time, i.e. the duration of the experiment. First of all, it is evident that these results do not reveal a growing trend throughout time. This can be explained by two different causes: either the sampling method fails to accurately and cleanly remove and identify the biofilm present on the plastic particles or the experimental circumstances and the plastic particles do not allow a significant growth. This last statement is backed up by the fact that in all three studied cases, there occurs a peak in ATP concentration around week 3 before dropping down again.

In terms of density measurement however, Figures 5.3 and 5.4 prominently reveal the inaccuracy of the method to measure the density of the plastic particles. The ranges of the standard deviation overlap so little can be concluded quantitatively in terms of the influence on the density due to the measured biofouling. Also, the measured density of the blank plastic beads (week 0) is in both cases lower than the value mentioned by the manufacturer (respectively 0.90 and 0.98 g/cm^3), indicating once more that the density measurement was too inaccurate for the purposes of this experiment.

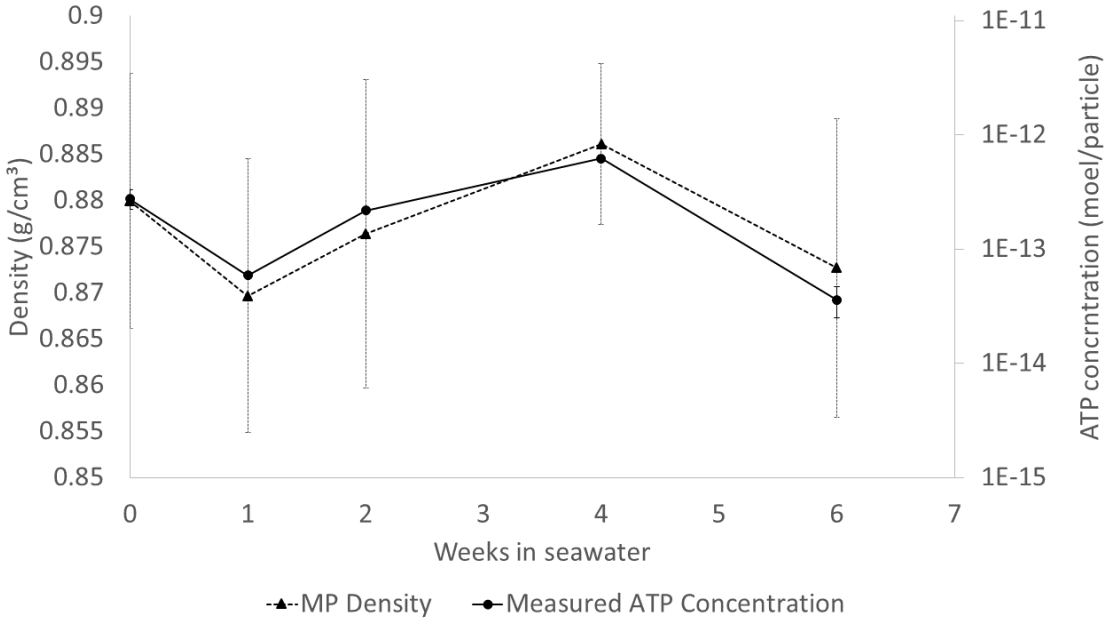

(a) *The results of the Biofouling 1 experiment for the PP particles throughout time. For weeks 0, 1, 2, 4 and 6 samples have been analysed for density and ATP concentration. The error bars represent the standard deviation between measurements of either density or ATP concentration. If n represents the number of repetitions per measurement, then n=10 and n=30 respectively.*

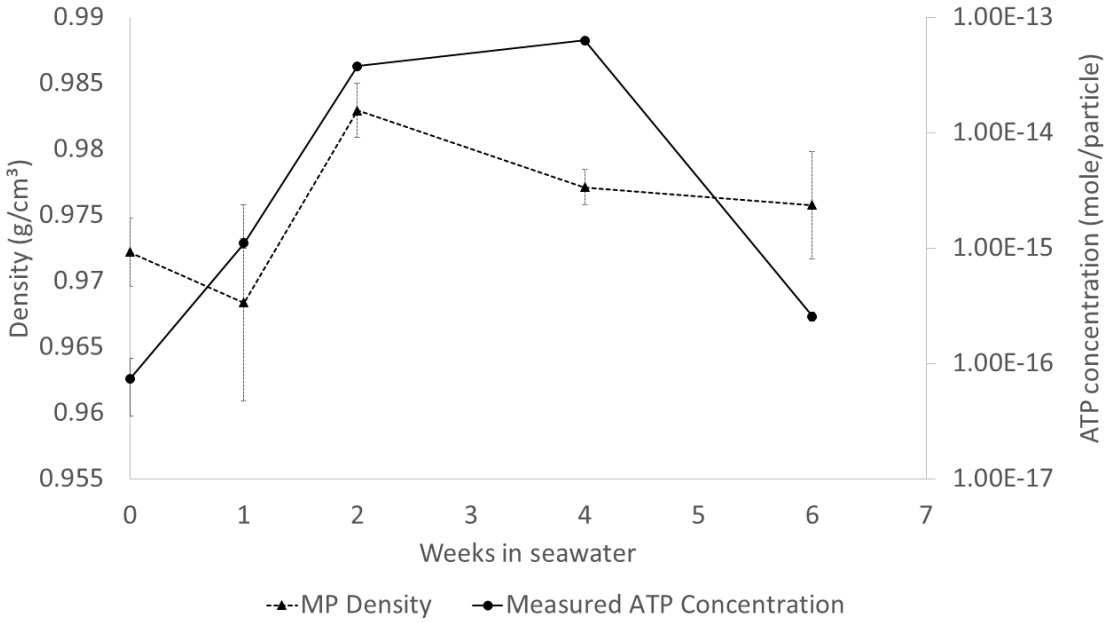

(b) *As for (a) but with the smaller PE particles. n=40 and n=30, for density and ATP concentration measurement respectively.*

Figure 5.3: *Results of the Biofouling 1 experiments for both the PP (a) and PE (b) beads.*

Lastly, Figure 5.5 shows the same results as Figure 5.3a for the PP particles but now the time factor is eliminated. Once again, it is clear that the vertical error bars, i.e. the deviation on the density measurement, are too big. Yet, the results show an apparent

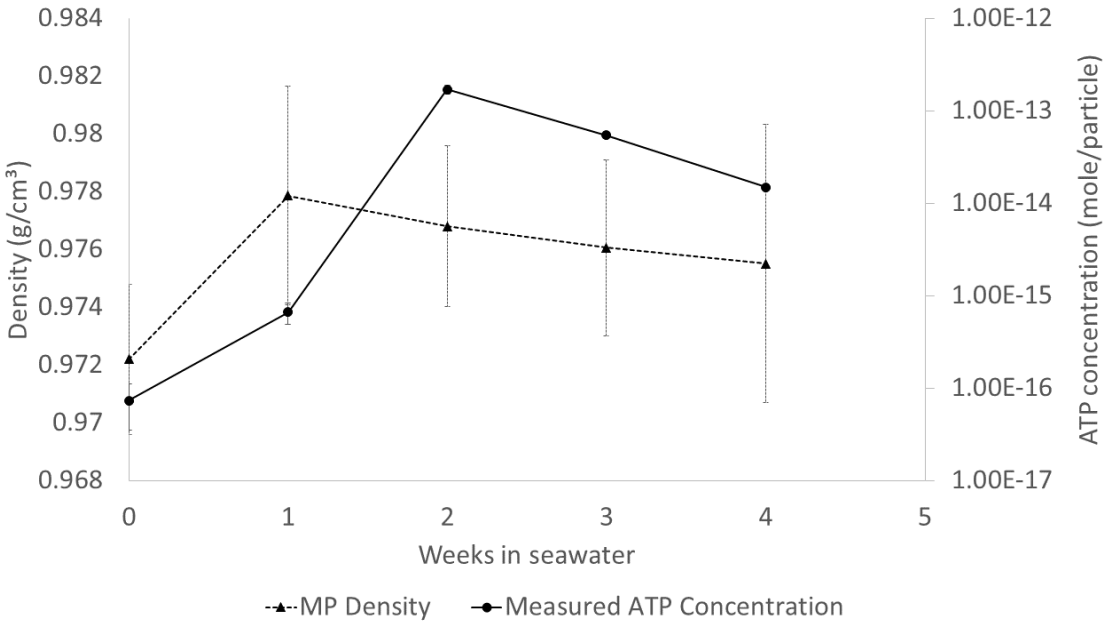

Figure 5.4: *The results of the Biofouling 2 experiment for the PP particles throughout time. For weeks 0, 1, 2, 3 and 4 samples have been analysed for density and ATP concentration. The error bars represent the standard deviation between measurements of either density or ATP concentration, If n represents the number of repetitions per measurement, then n=40 and n=60 respectively.*

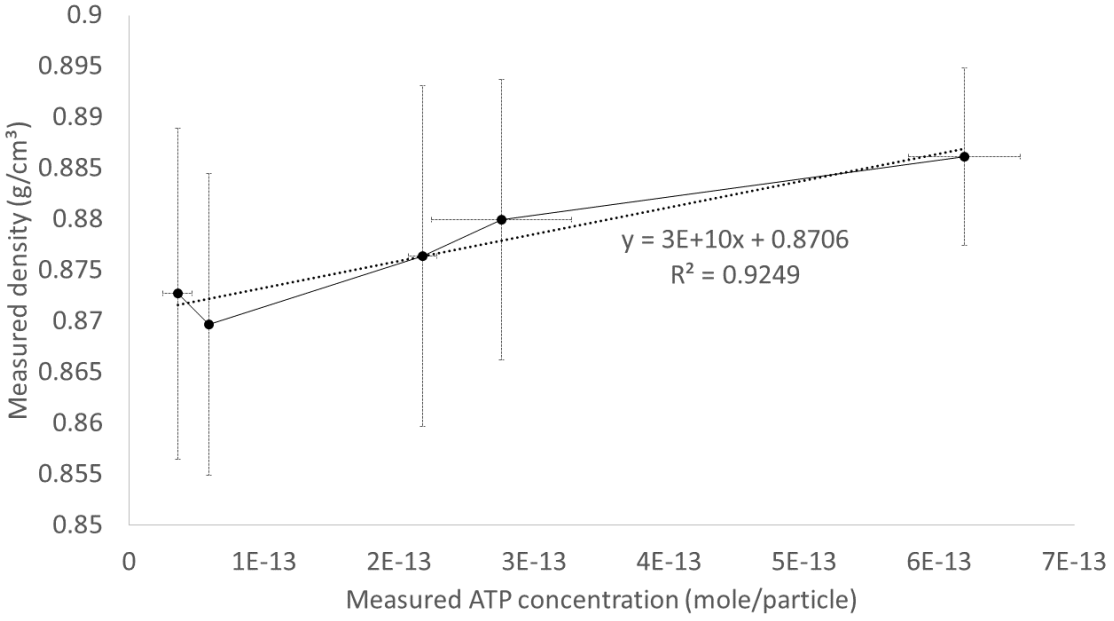

Figure 5.5: *This graphic present the correlation between measured ATP concentration and the particle density from the first experiment with PP particles (Biofouling 1, cfr. Figure 5.3a). The error bars represent the standard deviation between the set of repetitions of either variable: density (n=10) and ATP concentration (n=30). Also, the linear regression model between both variables is plotted (dotted line) and its coefficients are shown.*

correlation (R^2 = 92%) between particle density and the amount of biofouling. This is another indication, just as is mentioned in previous literature, towards the positive influence of biofouling on the density of a light (i.e. less dense than water) plastic particle. However, a quantitative description of this phenomenon, which is the goal of this experiment, cannot be supported by the obtained experimental results. Also, this apparent correlation between both characteristics cannot be identified for both experiments with the PE particles, only for the lighter PP particles.

5.3 SWRO Pretreatment Simulation

In order to discuss the results of the bench-scale pretreatment steps, a first section will more generally discuss the analyses that have been performed to evaluate a method that is essential to eventually analyse the results from the experimental part of this research. Secondly, these results of the different streams containing MP of both the DMF and the MF simulation will be presented and discussed. Finally, relevant mass balances of both pretreatment steps will be constructed and visually presented at the end of this chapter.

5.3.1 Quantification

1. Characterisation of the plastic beads

Before presenting the results of the simulated pretreatment steps it is essential to describe the MP used as spike for all the experiments. This forms the basis of the quantification of all obtained results. First of all, the PSD of the green PE particles is presented in Figure 5.6. The largest peak coincides with the size range as reported by the producer, the smaller peak is classified as a dust fraction. This fraction can be explained by either dust that systematically enters the analysis circuit or the presence of smaller plastic fragments due to physical degradation of the analysed MP. During the experimental part of this research, when the MP are handled, it is visually observed that the green PE particles are prone to physical degradation. In the end, from these measurements, every d_{50} is retained and an average value calculated: 101 ± 3 μm.

Given this average diameter and the density of the plastic particles, as reported by the producer (0.98 g/cm^3), a theoretical amount of particles can be related to a certain mass:

$$n_{MP} = \frac{m}{\rho V_{MP}} = \frac{6m}{\rho \pi d_{50}^3} \tag{5.1}$$

Where:

n_{MP} = Amount of MP particles (-)

m = Mass of MP (g)

ρ = MP particle's density (0.98 g/cm^3)

V_{MP} = Volume of an MP particle (cm^3)

d_{50} = Average diameter of an MP particle (cm)

This theoretical calculation allows a better description of the experimental conditions and will be necessary to further calibrate the counting methods. The first set of experiments, (MF1 and DMF1) is spiked with 3 mg green PE/L. Theoretically, this relates to an average concentration of 5 675 ± 169 MP/L. The second set of experiments (MF2 and DMF2) is spiked with 0.3 mg green PE MP/L, or an average spike concentration of 567 ± 17 MP/L. The first spike is chosen this high to lower the relative amount of MP lost throughout the experiments and to be able to observe differences between the different resulting streams. After this first set of experiments, a repetition is performed with a lower concentration, one that would still be quantifiable during the experiments but one that, at the same time, also approaches more realistic concentrations, as mentioned in 2.1.2.

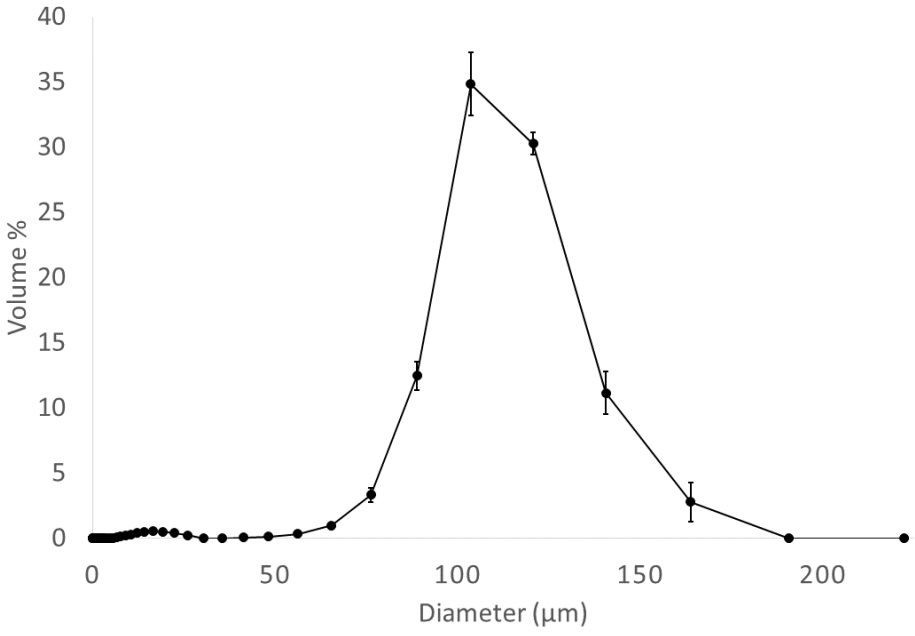

Figure 5.6: *PSD of the green PE particles (reported size: 90-106 µm) which is used as spike in all the bench-scale pretreatment simulations. The error bars represent the standard deviation (n = 10). The small peak around the particle size of 15 µm that occurs in all repetitions can be explained as a dust fraction present in the system.*

2. Calibration of the counting method

This calibration covers the relation between the amount of pixels present on a microscope picture and the isolated pixels using the processing method as described in Section 4.2.6. 20 pictures with an amount of particles that is feasible to count by hand are selected, counted and then processed using the chosen settings. This calibration gives rise to an average value of 62 ± 9 pixels (Y) per particle (X):

$$Y = (62 \pm 9)X \tag{5.2}$$

The selected pictures contain 5 pictures from the standard series (clean), 10 other clean pictures (clean) and 5 pictures from backwash or column analysis (dirty). It is clear from Figure 5.7 that there is some variation due to this method of counting particles, which is reflected in the relative error of 9/62 = 15%. This relationship will further be used in the analysis of the results from the different streams in the bench-scale pretreatment simulation.

In a first phase of analysing these resulting filters, it is observed that the spread of MP on the filter is very heterogeneous. This is a first indication that estimating the amount of MP present on every filter will be a challenge during this research, as the heterogeneity leads to very high uncertainties when an average is calculated. Therefore, a sensitivity analysis is performed on 20 resulting filters from the first ex-

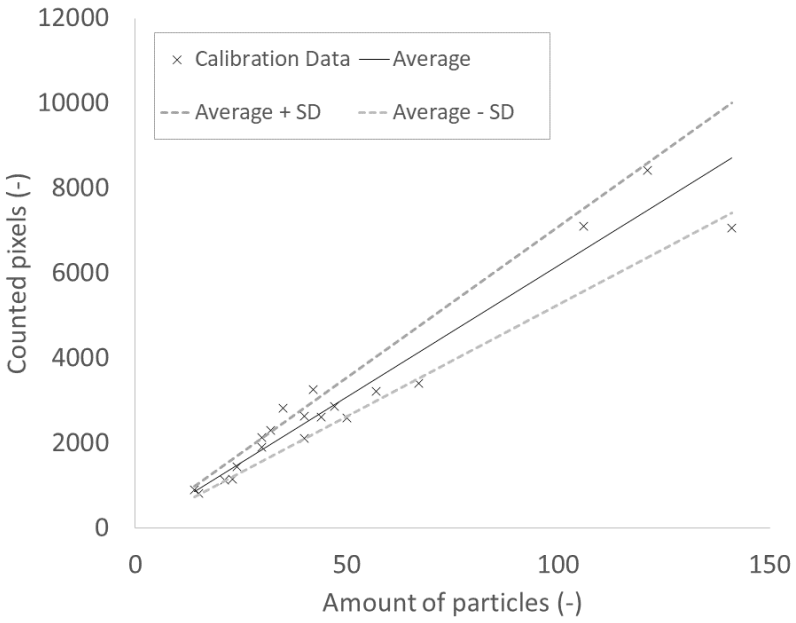

Figure 5.7: *Visual representation of the calibration series to determine a relationship between the amount of green particles present on a filter and the counted pixels using ImageJ. The average value of 62 ± 9 pixels per particle is also plotted, with an upper and lower boundary based on the standard deviation (n=20).*

periment, being the first MF set-up (MF1 in Table 4.3). This method, "Method 1", is initially proposed to estimate the amount of MP by taking a series of microscopic pictures with a known surface area, average the result and transform this average to an average for the entire filter. This was possible as the surface area of the filter is known (90mm diameter or 6 362 mm^2) and the exact surface of the microscope picture is known (384 mm^2), as all pictures are taken at the same height and with the same magnification: x10x0.63. The sensitivity analysis evaluates the evolution of the standard deviation in function of the amount of pictures taken. It is proposed that a higher amount of pictures would lower the variability of the outcome. However, the heterogeneity does not allow the variability to decrease as can be derived from Figure A.1 in the Appendix section of this paper. The backwash filters visually show a more heterogeneous spread than the influent filters and this is also reflected in this analysis: the 4 filters with the highest relative standard deviation (black, full lines) are all backwash filters. Either way, standard deviations of over 100% do not allow an accurate estimation of the results of the experiments and this already indicates that this method is insufficient to quantify the results of the performed lab-scale experiments during this research.

3. Standard Series

As a result of this observation, the next step is the construction of a standard series with the green MP. The standard series consists of 12 samples, which are the same filters used during the experiments on which an accurately weighed amount of MP has been transferred heterogeneously in order to be representative for the experimental results. This series is then analysed using the above mentioned Method 1 (i.e. averaging the estimated amount of MP on random pictures (20)) as well as with the new method, Method 2, as described in Section 4.2.5, where the filters are divided in specific zones and all zones are covered by pictures, cut out digitally and eventually processed with ImageJ to count the pixels of green particles. In the end, this procedure allows to construct a calibration curve that relates the counted pixels by the method to a theoretically expected number of particles of the 12 standard filters. This allows a quantitative insight in the accuracy of both methods. The data on which this calibration is based are given in Table 5.1. The lower boundary for this standard series is determined by the accuracy of the weighing method, the upper boundary is determined by the fact that the filters from the experiments contain MP up to an order of magnitude of 10 000 particles.

On the one hand, this calibration reveals the strong deviation of the estimated amount from the theoretically expected amount when using Method 1. Figures 5.8a and 5.8b show how the estimated values gradually overestimate the expected amount and the increasing relative error of the method when the filters contain more and more MP. As a result, this method is not only characterised by a high variability, as seen in Figure A.1, but is also positively biased.

Table 5.1:
The 12 calibration points used to evaluate the accuracy of a counting method to estimate the amount of MP present on a filter. The theoretically expected amount is the result of converting the weighed mass to a number using the average value for d_{50} (cfr. above).

Mass of MP (mg)	Theoretical number of MP (-)
0.471	856
0.955	1 735
1.519	2 759
2.043	3 711
2.442	4 436
3.087	5 608
3.529	6 411
4.028	7 317
4.335	7 875
5.087	9 241
5.652	10 268
6.212	11 285

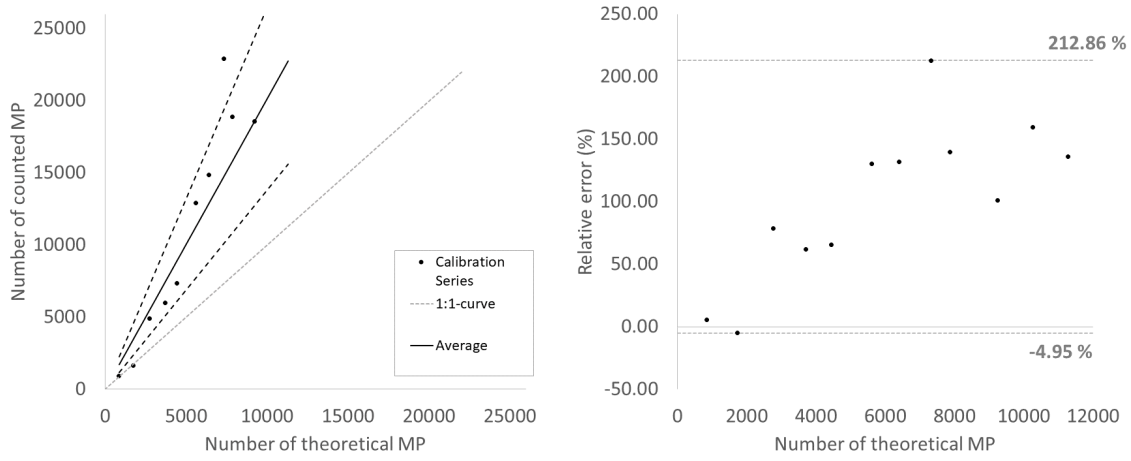

(a) ***(b)***

Figure 5.8: *Visualisation of the analysis of Method 1 based on the standard series: (a) shows the deviation of the result from the theoretically expected value. The average value of this deviation is plotted with an upper and lower boundary (black dotted curves) based on the standard deviation between the estimated values by Method 1. The grey dotted line is the 1:1 curve, which represents the ideal case in terms of approaching the theoretical value. The error bars on the estimated values have been omitted in this figure since they would cover the entire graph area given the high variability, as established in the previous analysis of this method (cfr. Figure A.1). (b) sets out the relative error between the estimated amount of MP by Method 1 and the theoretically expected values from the standard series. The grey dotted lines show the maximum deviation, both in positive sense (i.e. overestimation) and negative sense (i.e. underestimation). (SD = standard deviation)*

On the other hand, this analysis demonstrates that Method 2 does not consistently overestimate the result (Figure 5.9a). Mind the difference in y-axis values between Figure 5.8a and Figure 5.9a, as the estimated values from Method 1 deviate much more from the expected value than the estimated values from Method 2. The error relative to the theoretically expected value is smaller and varies positively and negatively (Figure 5.9b) This indicates that this method is not biased and results in a smaller variability between results. Eventually, despite the labour/accuracy trade-off, this most accurate and less variable method, i.e. Method 2, is selected to analyse the results of all experiments performed during the simulation of the SWRO pretreatment steps. The standard curve in Figure 5.9a results in an average relation of 1.01 ± 0.26 between the estimated amount of MP (X, from 5.2) and the theoretically expected amount of MP (Z):

$$X = (1.01 \pm 0.26)Z \tag{5.3}$$

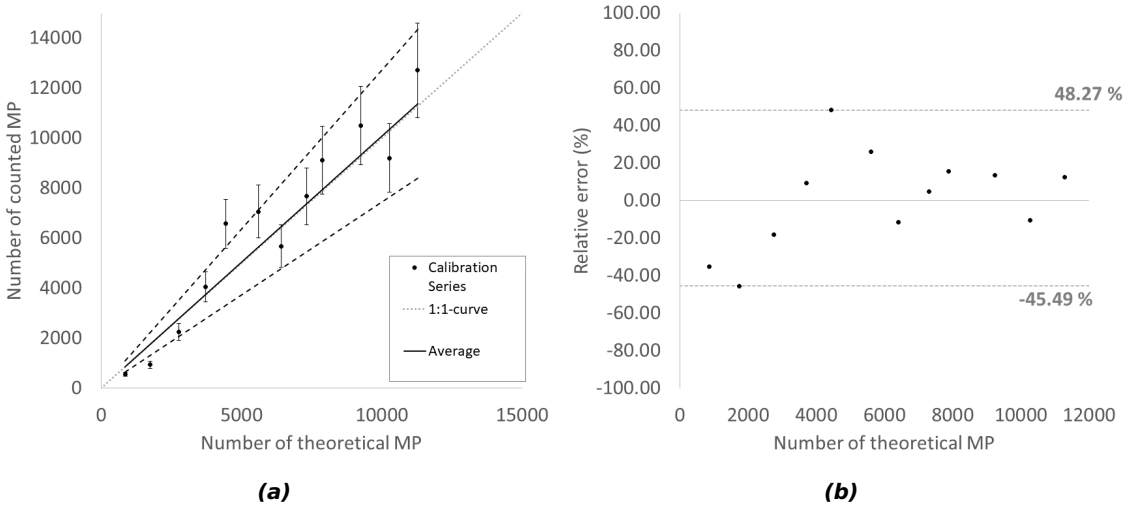

(a) ***(b)***

Figure 5.9: *As in Figure 5.8, these graphs visualise (a) the deviation from the theoretically expected value in the standard series. The error bars represent the standard deviation as a result of the pixel-particle calibration (Figure 5.7). Subfigure (b) visualises the relative error on the standard series for Method 2: the relative deviation of the counted amount of MP from the theoretically expected amount. (SD = standard deviation)*

By doing so, both the error derived from the pixel-particle relationship (Equation 5.2) as well as this error derived from the standard series curve for Method 2 (Equation 5.3) will be taken into account to determine and quantify any result obtained using this method. In what follows, the results from the experimental set-ups to follow up the fate of MP in pretreatment steps are a product of both calibration curves. The corresponding error reported with these results is the combined standard deviation as an error on the estimates, which is then defined as the sum of the individual relative errors: 9/62 + 0.26/1.01 = 15% + 26% = 41%.

5.3.2 Dual Media Filtration

DMF Influent

As mentioned in the previous chapter (Section 4.2.1), empty column runs are performed to better estimate the actual flux of MP that passes through the constructed system, rather than relying on the mass of MP that is added as spike to the feed tank. For both the DMF1 and DMF2 experiments (spiked with respectively 3 and 0.3 mg MP/L, cfr. Table 4.3), 1 empty run of 100L was performed. This results in an average ingoing flux of 5 491 ± 2 249 and 676 ± 277 MP/L, respectively. These values will further act as the reference influent concentration to define removal efficiencies and corresponding mass balances.

DMF Effluent

One of the main interests in this research is to identify the pretreatment steps that retain MP during their operation. All effluent filters appear to contain little to none MP after visual inspection, which implies that the result is counted by the naked eye using a microscope. The results are listed in Table 5.2. The removal efficiencies of the spiked green MP during both DMF experiments reach 99.9%. In a previous study with the combination anthracite-sand no breakthrough was observed, however,in this case, only a 2L spike was fed to the filter. After the long-term operation of 10 days in this study, a minimal breakthrough of MP is observed, which is in line with the previous finding [68]. Mind that both DMF experiments have been performed with fresh filter material (anthracite and sand) as it is removed after each experiment for the analysis of the filter material itself.

In Section 4.2.1, it is mentioned that in the second experiment (DMF 2), an additional spike of 0.3 mg/L of white MP is added to the influent of the DMF set-up. These white MP are smaller than the green MP spike, with a reported size of 10 to 45 μm. As no method is developed to accurately count these MP in the resulting streams, their quantification is no goal of this experimental research. However, 2 times 1L of every run of 100L is collected over black filter paper to be used for a qualitative indication for breakthrough of these smaller MP. However, on none of the 10 (2x5) black filter papers from this experiment a white MP is found after microscopic analysis. Without any further ground for conclusions, this is an indication that smaller MP, with a size range close to the lower boundary of MP, are possibly also well retained by the DMF set-up. This will be further discussed at the end of this study in Section 7.1.

Table 5.2:
Overview of the analysis of the effluent filters for both DMF simulation experiments (1 run = 100L). The removal efficiency per run is expressed as a fraction of the average influent of the DMF 1 and the DMF 2 experiments, respectively 5 491 and 676 MP/L. The number of MP in the second column are counted manually and no standard deviation is reported for those values. (SD = standard deviation)

Run	Number of MP (-)	Concentration (MP/L)	Removal Efficiency (%)	SD (%)
DMF 1				
1	5	0.05	99.999	± 0.0004
2	3	0.03	99.999	± 0.0002
3	56	0.56	99.990	± 0.0042
4	19	0.19	99.997	± 0.0014
5	42	0.42	99.992	± 0.0031
Average	**25**	**0.25**	**99.995**	± **0.0093**
DMF 2				
1	30	0.30	99.956	± 0.018
2	3	0.03	99.996	± 0.002
3	2	0.02	99.997	± 0.001
4	1	0.01	99.999	± 0.001
5	0	0	100	± 0.001
Average	**7.2**	**0.072**	**99.989**	± **0.022**

DMF Backwash Procedure

After each of the first 4 runs out of 5 in total of every DMF experiment, a backwash procedure is performed. The resulting backwash stream with washed out contaminants and MP is again collected on filters. Given the design parameters, a backwash procedure lasts 10 minutes and 6L of water is sent bottom-to-top through the column, which is eventually collected on a series of 6 filters (i.e. 1L is passed over each filter). Figure 5.10 visualises these 8 backwash procedures: 4 times for each experiment (respectively 5.10a and 5.10b). The values are expressed as the fraction of the total amount of MP that is washed out during each procedure (i.e. all 6 bars of a certain backwash add up to 100%). These results show that most of the washed out MP detach from the filter material easily. In 6 out of 8 cases, observed over both experiments, at least 50% of the total amount washed out during a backwash procedure is removed in the first minutes, contained in the first litre of backwash water.

In response to Figure 5.10a (DMF 1), two additional remarks are necessary. First of all, during the very first procedure ("Backwash 1" in DMF 1, black bars), the backwash is performed poorly. The filter material does not expand and the water passes through the filter material as if it were a regular sand filter. This explains the more uniform washing out of the MP that can be observed. Also, as will be shown in Table 5.3, the total amount of MP washed out is the lowest during this backwash procedure, indicating its poor execution compared to the other backwash procedures.

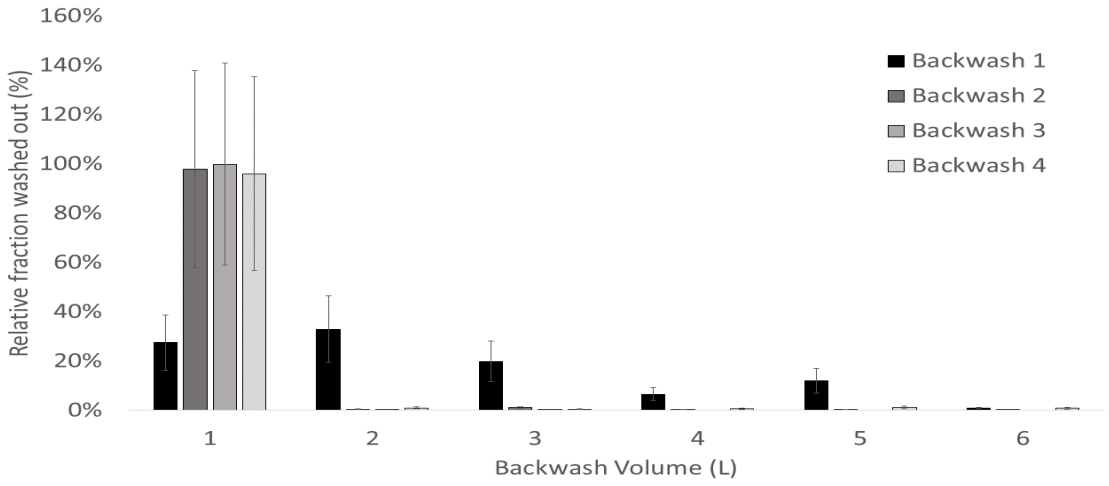

(a)

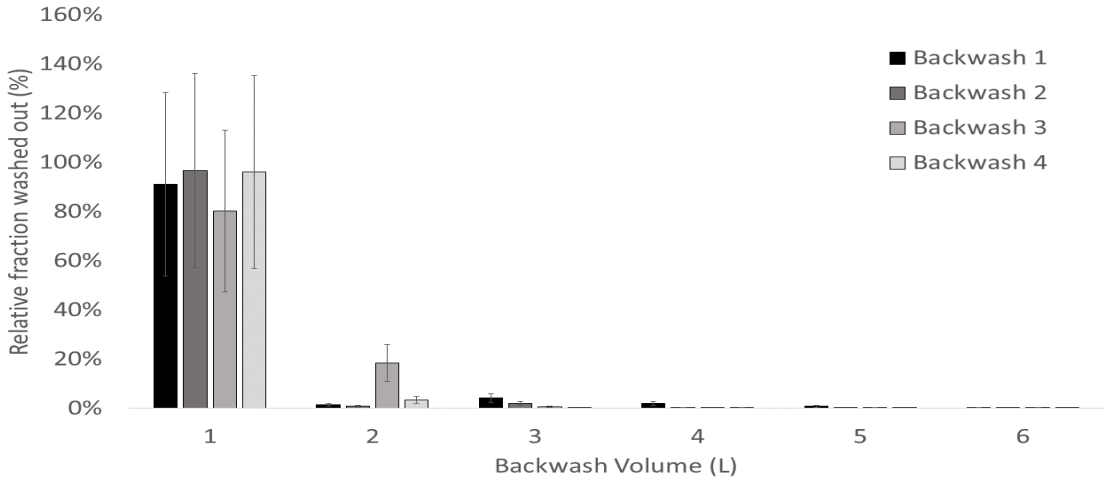

(b)

Figure 5.10: *Overview of the amount of MP removed during each backwash. The values are expressed as the fraction of the total amount of MP washed out during each individual procedure (i.e. all 6 bars of each set add up to 100%). The results of each of the 4 backwash procedures for both experiments (4*2=8) are presented, respectively (a) DMF 1 and (b) DMF 2. The 3rd backwash of DMF 1 lacks measurements for 4, 5 and 6L as the procedure was disrupted due to technical issues.*

Secondly, due to technical issues, no analysis of the second half of the 3rd backwash procedure (4, 5 and 6L) has taken place. However, the trend in the other procedures is that the majority of MP is already removed from the filter material in the first litres of backwash. This allows to assume that only a very small fraction will probably have gone undetected because of this.

In absolute terms, the results between the repeated backwash procedures are more variable (Table 5.3). This is also dictated by the high variability inherent to the counting methods employed during this research, which can be observed in the big inter-

vals on the estimated amounts of MP. The difference in order of magnitude between the 2 experiments (DMF 1 and DMF 2) reflects the 10-fold difference of ingoing concentration of the green MP for both experiments. The lowest value is observed in the first backwash procedure and can be explained by the fact that this backwash is performed poorly, leaving still many MP attached to the filter material. On the other hand, a removed amount higher than what is sent over the DMF column during 1 run is observed during 2 backwashes (DMF 1-3 and DMF 1-4), i.e. more than 100%. This can be explained by the build-up of MP because of the poor backwash at the beginning of the experiment. A more detailed description of the progress of the experiments, covering all different runs and backwashes as one system, will be presented in Section 5.3.2. However, before constructing such a mass balance over an entire experiment, the results from the column analysis are essential. This will determine the amount of MP that are still left in the system at the end of both DMF experiments. In other words, this will represent the fraction of spiked MP that has not been washed out over the course of an entire experiment.

Table 5.3:
Overview of the analysis of the backwash filters for both DMF simulation experiments (1 run = 100L). Here, the backwashed fraction is the total amount washed out expressed as a fraction of the average influent of the DMF 1 and the DMF 2 experiments, as determined by the empty column runs: respectively 5 491 and 676 MP/L. This means it is only calculated with reference to 1 run of 100L. (SD = standard deviation)

Backwash	Number of MP (-)	SD (-)	Fraction (%)	SD (%)
DMF 1				
1	100 815	± 41 286	18	± 8
2	198 617	± 81 338	36	± 16
3	636 962	± 260 848	116	± 50
4	650 883	± 266 549	119	± 51
DMF 2				
1	41 173	± 16 861	61	± 26
2	25 471	± 10 431	38	± 16
3	14 255	± 5 838	21	± 9
4	34 142	± 13 982	50	± 22

Column Analysis

After the final 5^{th} run, no backwash is performed. Instead, the filter material itself is removed from the column and analysed for the MP it contains. In contrast to the backwash, this gives an indication of the vertical distribution of the spiked MP. As the measurement of MP in the effluent of the DMF set-up in Section 5.3.2 points to an almost complete removal of the spiked MP from the incoming stream, this column analysis gives additional insights to further study and discuss the behaviour of MP in SWRO pretreatment. The results of this analysis of both DMF columns are presented in Figures 5.11 and 5.12. This analysis is destructive, so it can only be done at the

end of an experiment. Therefore, in parallel with the previous results, by means of a qualitative indication, the deepest visually discernible green MP in the column is also searched for and its depth is measured every 1.25h of operation (i.e. every 10L). The average of the 5 runs that form 1 experiment are both presented in Figures 5.11 and 5.12. The analysed column has been divided in 10 segments, segment 1 is the top of the column (anthracite), segment 10 is the bottom segment (sand).

First of all, the measurement of the deepest green particles, i.e. the visual MP front, appears to be a good qualitative indicator to identify the lower boundary of the bulk of MP present in the filter material. In both cases, the segment of the deepest visual MP and the segments above contain more than 99% of the total MP retrieved after the destructive analysis of the filter material. Secondly, during both experiments more than 90% of the total MP retrieved inside the filter material at this point in time are found in the top 2 segments. However the relative distribution differs between both experiments. In DMF 1, the experiment with the highest spike concentration (3 mg MP/L) the difference in distribution between the top segment and the second segment is less strong than in DMF 2 (0.3 mg/L). For the first experiment, the top layer contains 55 ± 23% of the MP and the second layer 39 ± 16%. For the second experiment, the distribution is 85 ± 30% and 13 ± 5%, respectively for the 1^{st} and 2^{nd} segment. The 3^{rd} segment also harbours a larger relative fraction in the first experiment (6 ± 2%) than in the second experiment (2 ± 1%). In the second experiment, it can be seen that in some segments not even 1 MP was retrieved, more specific segments 5, 7 and 10, while this is not the case for the first experiment. As the influent concentration is higher in the first case, the progress of the green MP goes deeper after the duration of the experiment (500 L) than in the second case, where the incoming MP concentration is about 10 times lower. The visual indicator also points in this direction, with the visually present MP found deeper in the material for DMF 1 compared to the result for DMF 2, down to 26.4 and 19.8 cm respectively. Thirdly, this vertical distribution shows that the bulk of the retained MP are present in the top layer of anthracite material, very little of the retrieved MP are found in the bottom layer of sand.

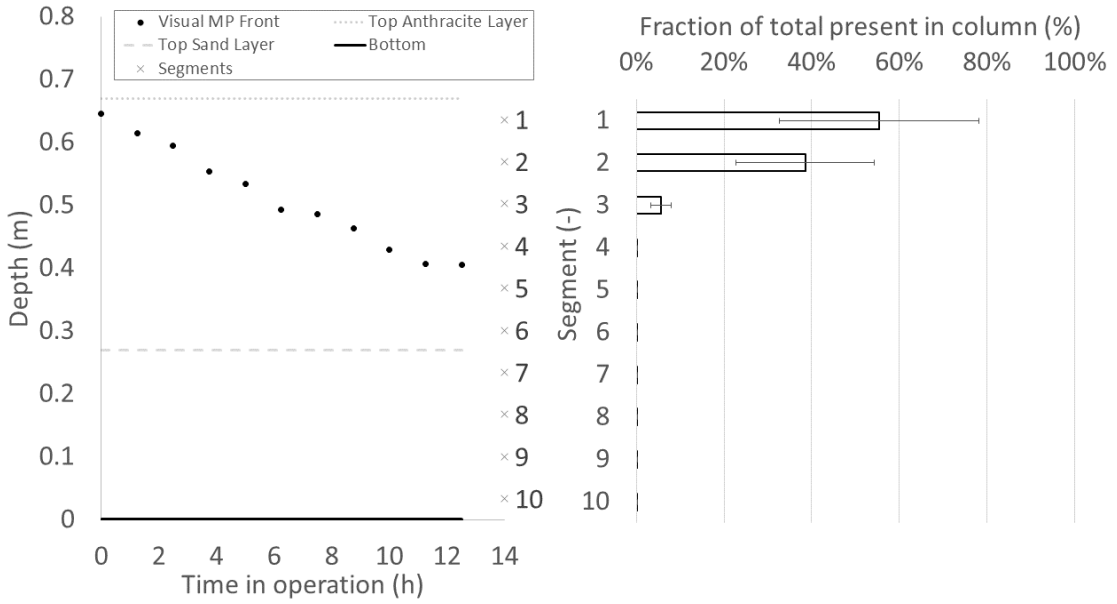

Figure 5.11: *Visualisation of the vertical distribution of MP throughout the DMF filter material, for the first experiment (DMF 1). The right graph shows the amount of MP found in each segment of 6.7 cm of the filter material itself, at the end of the experiment. The values are expressed as relative to the total amount retrieved in the entire column (i.e. the fractions of all 10 segments add up to 100%). The left graph shows the visual progress of the green MP, which was recorded during operation, to verify if this measurement were a good indicator of the presence of the green MP in the filter. The y-axes of both graphs correspond with each other (e.g. segment 1 corresponds with the top 6.7 cm on the left). Both graphs represent results from experiment DMF 1 (3 mg MP/L).*

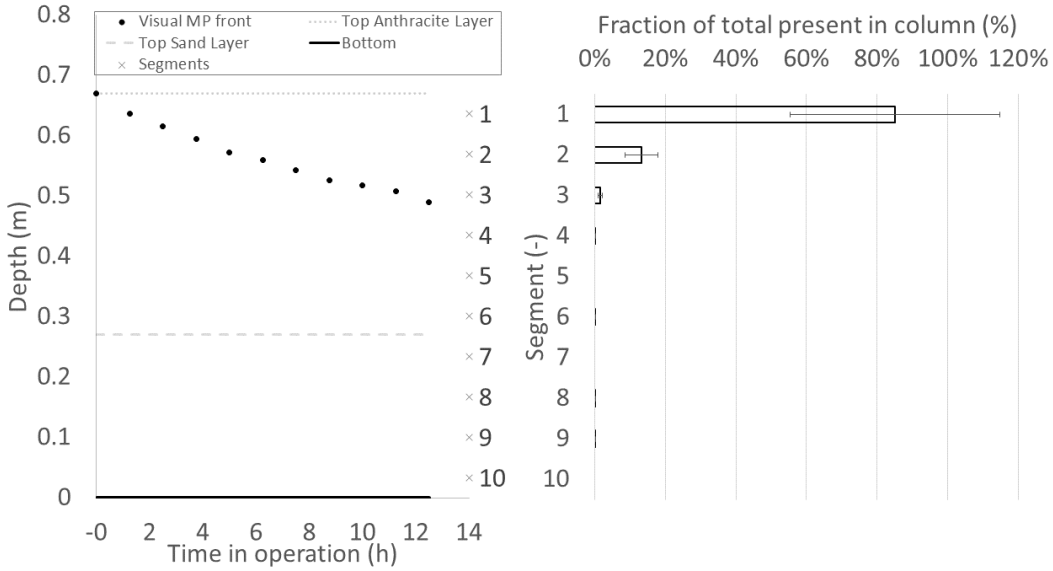

Figure 5.12: *As in Figure 5.11, the right graph shows the relative amount of MP present in each segment of the DMF column and the left graph shows the visually measured progress of the green MP, both for experiment DMF 2 (0.3 mg MP/L). For segments 5, 7 and 10, no MP are found and the result is 0.*

DMF Mass Balance

Finally, all results from the experimental research are collected to construct a mass balance over the DMF system. The 2 DMF experiments are schematically represented in Figures 5.13 and 5.14. The 5 elements in the DMF mass balances are of course always the same column but they represent the progress of the experiment through time. The inputs for every run are the influent and the residual MP from the previous run. These residual MP comprise the MP that have not been flushed out during the previous backwash and the MP that went undetected in previous outgoing streams. In other words, the residual fraction is a conservative calculation as not necessary all undetected MP are still present in the system, they may have gotten physically lost during the process (e.g. stickiness of tubing or fittings). The outputs of every run are the effluent stream, the backwash stream and the residual fraction that remains in the system. In the end, an additional output is present: the column analysis at the end of each experiment. The first backwash (DMF 1, Run 1) is performed poorly, without expansion of the filter material. The remaining backwashes are performed better and all in the same way.

This representation of the results is particularly interesting to interpret the backwash efficiencies of the DMF systems. As the filter material stays in place for a following run, and not 100 % of the MP has been removed during the intermittent backwash cycle, a fraction of the MP that are originally form the previous run are still present in the system can either break through or be washed out during the next runs. If this is not taken into account, the calculation of backwash efficiencies solely based on the influent concentration would lead to an overestimation (cfr. the backwash recovery of over 100% in Table 5.3). Now, from this point of view, the backwash efficiencies for the DMF system range from 10 ± 4 % to 61 ± 26 %, conservatively, i.e. when all residual MP are assumed to remain within the system. Given the broad range of results, there is no ground to state a significant difference between the 2 DMF experiments. Respectively, there is an average removal of 34 ± 14% and 29 ± 12% of the ingoing MP after every backwash.

A final remark is made on the large fraction of MP that remains undetected during the analysis, named the "Residual" fraction, which is revealed by constructing these mass balances. This shows that the experimental method is unable to trace back every MP that is part of the experimental design, for which there are various explanations: (1) the plastic particles can get stuck in the system, for example due to stickiness of the tubing or the used fitting; (2) the removal of the MP during the column analysis was not 100% and some are still present in the removed filter material DMF; (3) and, as observed throughout the analysis of the results, the counting method is characterised

by a relatively large margin of errors which may explain the importance of the residual fraction as the sum of MP in the resulting streams does not add up to 100% due to these counting errors. The residual fractions over the total experiment of 5 runs of DMF 1 and DMF 2 are 20 ± 8% and 53 ± 22% respectively. These are calculated as the absolute amount of MP in the final residual stream (i.e. after the 5^{th} run in Figures 5.13 and 5.14) divided by the total ingoing spike of MP, which is 5 times the influent amount in the overall mass balances.

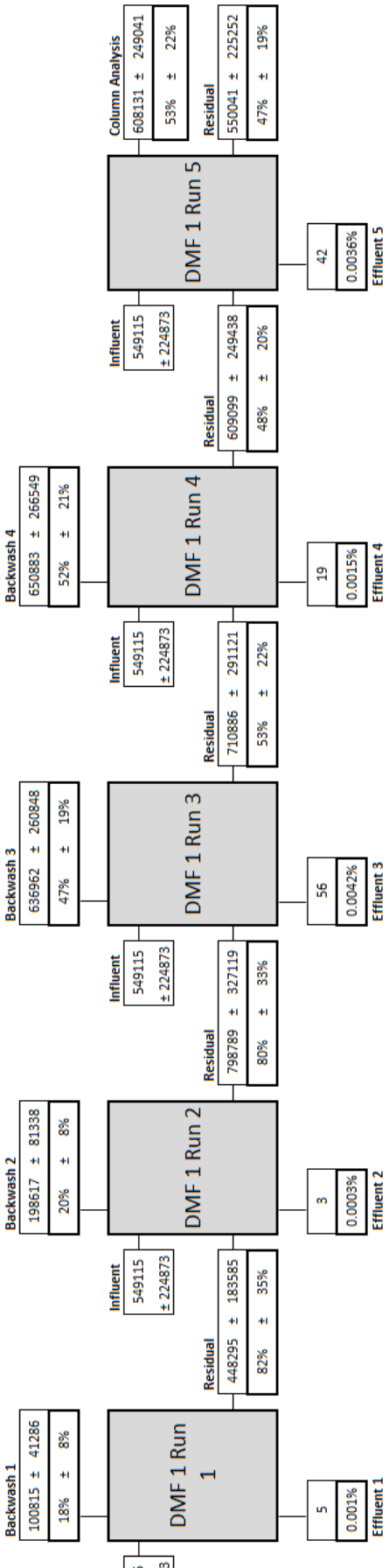

Figure 5.13: *Overall mass balance of the DMF 1 experiment. The percentages are the relative amount present in a certain output (either backwash, effluent or residual). Residual is the amount that is not retrieved in the other outputs. Every balance is made over every element (i.e. one of the experiment's runs). Only the residual fraction transfers to the next element and acts as a second input, additional to the spiked influent. All errors are reported as standard deviations. Effluent filters are counted manually = no standard deviation.*

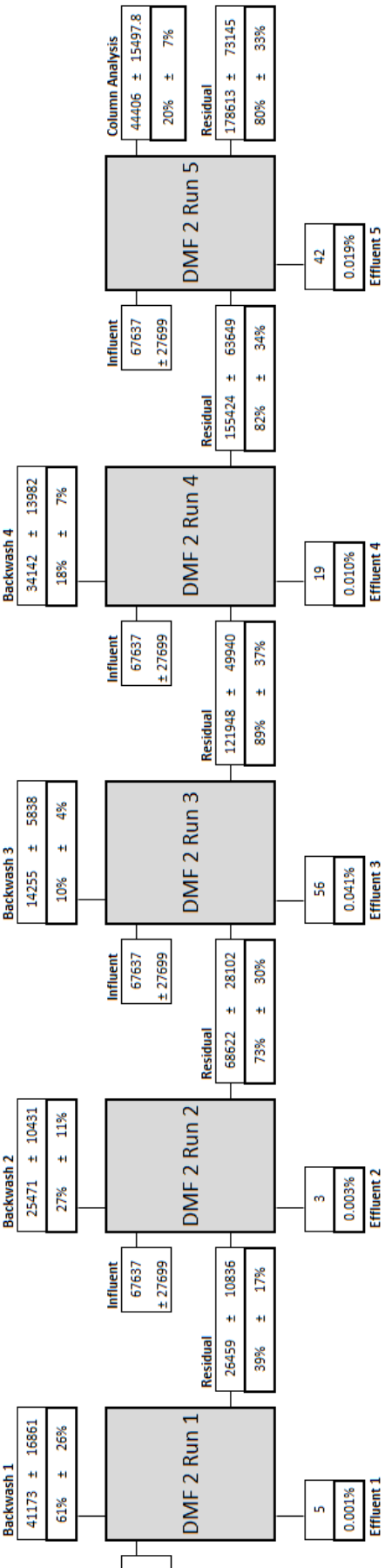

Figure 5.14: *Overall mass balance of the DMF 2 experiment. The percentages are the relative amount present in a certain output (either backwash, effluent or residual). Residual is the amount that is not retrieved in the other outputs. Every balance is made over every element (i.e. one of the experiment's runs). Only the residual fraction transfers to the next element and acts as a second input, additional to the spiked influent. All errors are reported as standard deviations. Effluent filters are counted manually = no standard deviation.*

5.3.3 Microfiltration

MF Influent and Effluent

As in the DMF experiments, an empty column run has been performed for the MF cartridge. This results in an average influent concentration of 5 610 ± 2 297 MP/L and 749 ± 307 MP/L, for MF1 and MF2 respectively. These values are comparable with the parallel DMF experiments, which is expected as the same mass of MP is being added to the influent, 3 mg MP/L and 0.3 mg MP/L. The respective removal efficiencies for both experiments amount to 99.986 ± 0.006% and 99.993 ± 0.003%. This result is comparable with what is found in a WWTP sampling campaign, where an MF membrane process is reported to remove 99.1% of the incoming MP [64].

During the second MF experiment (MF2), an additional spike of 0.3 mg/L of white MP is added to the influent of the MF set-up. As in the second DMF experiment, 2 times 1L of effluent is collected over black filter paper to be used for a qualitative indication for breakthrough of these smaller MP. However, on neither of black filter papers from this experiment a white MP is retrieved after microscopic analysis, as in the DMF set-up. Similarly, this is also an indication that smaller MP, with a size range close to the lower boundary of MP, are possibly also well retained by the MF membranes.

MF Backwash Procedure

After the experiment, the MF membrane is backwashed as well. In practice, this is done to counter membrane fouling but typically already after a shorter duration of filtration (cfr. Table 4.2). However, no significant pressure drop is observed during

Table 5.4:
Overview of the MP measured in each stream from both MF experiments. As before, the MP fractions are expressed as a fraction of the total ingoing MP (influent). SD = standard deviation. The effluent filters are counted manually = no standard deviation.

Type	Number of MP (-)	SD (-)	Fraction (%)	SD (%)
	MF 1			
Influent	336 591	± 137 840	-	
Effluent	48		0.014	± 0.006
Backwash	84 735	± 34 700	25	± 10
Residual	251 808	± 103 120	75	± 31
	MF2			
Influent	44 953	± 18 409	-	
Effluent	3		0.007	±0.003
Backwash	23 333	± 9 555	52	± 21
Residual	21 616	± 8 852	48	± 20

the experiment and there was no need to immediately backwash the MF module. In the end, the backwash procedure is executed with a fraction of the permeate that is sent back in the other direction, in this case outside-in. The backwash procedure has lasted longer than is typically done in practice (6 minutes as opposed to 2 minutes), however 95% of the retrieved MP are already removed in the first 2 minutes for the first MF experiment. In the second experiment, where the relative amount retrieved in the backwash stream is higher (52% of the influent as opposed to 25% in MF1, cfr. Table 5.4), it takes 4 minutes before more than 95% of the backwashed MP is washed off from the MF membrane.

Nevertheless, the total recovery of MP from the MF membrane is not that high. Table 5.4 shows that only 25 ± 10% and 52 ± 21% of the total ingoing MP have ended up in the backwash stream, leaving a large fraction (75 ± 31% and 48 ± 20%, respectively) undetected or stuck in the MF membrane. The latter can be visually verified as there are still green MP visible on the white MF membrane in the module. All results from both MF experiments are also visualised by means of a mass balance in Figures 5.15a and 5.15b. The MF mass balances consist of the influent as input and the effluent, backwash and residual fraction as output.

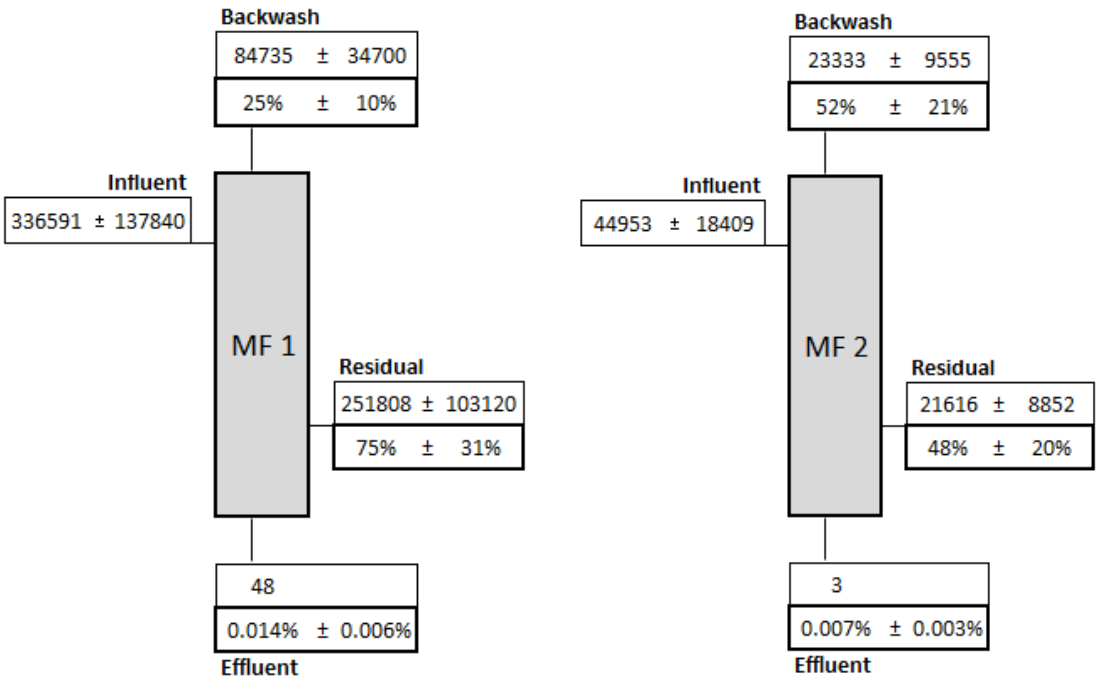

(a) *MF 1: Mass balance*

(b) *MF 2: Mass balance*

Figure 5.15: *Overall mass balances of both MF experiments, respectively (a) MF1 and (b) MF2. The percentages are the relative amount present in a certain output (either backwash, effluent or residual). The only input of MP is the spiked influent. Residual is the amount that is not retrieved in the other outputs. All errors are reported as standard deviations. Amount of MP in effluent streams is manually counted = no standard deviation.*

CHAPTER 6

PLASTIC FLUX SIMULATION

6.1 Plastic Flux

In the final part of this research, a desktop study is performed to estimate the amount of MP that may pass through a full-scale SWRO installation. At first, a preliminary estimation is worked out to get an idea of the orders of magnitude of the sketched situation. Secondly, based on this estimation and also using the results from the experimental part of this research, various scenarios are studied by making mass balances over a general SWRO installation to predict the hotspots where incoming MP are separated and in which streams they end up. For estimation purposes, characteristics from the earlier described large-scale plant (Ashkelon (Israel), cfr. Table 2.2) are used.

The first calculations consider the total plastic flux through an SWRO system, regardless of separation steps and efficiencies. The MP concentration is derived from literature. As described in Section 2.1.2, the studies mentioned in Li et al. [6] that use a fine sampling method (down to 50 μm) and are performed in coastal areas, where the intake system of an SWRO installations is also located, report MP concentrations in the order of magnitude of 1 000 to 10 000 MP/m^3 [20,21]. Therefore, a concentration of 1 MP/L (1 000 MP/m^3) is selected. This assumption is also supported by the expert knowledge of Prof. Dr. Colin Janssen (University of Ghent). It is obvious that exact concentrations are hard to pin down and that such estimations are subject to a high degree of uncertainty. Therefore this estimation is in the first place presented as an attempt to create a first idea of the order of magnitude of the studied phenomenon. Further assumptions include: 100% of the MP entering the water intake system of the SWRO installation pass through the entire installation; the average mass of an MP particle is set at 0.005 mg/item, which was also derived as an average from reported findings of MP in natural samples [6,11,19]. The plastic particle flux is then calculated using:

$$Plastic\ flux\ \frac{kg}{d} = C_{MP} * m_{MP} * Q * 1000 \frac{L}{m^3} * 10^{-6} \frac{kg}{mg} \tag{6.1}$$

Where:

C_{MP} = MP Concentration (MP/L)

m_{MP} = Mass of MP (mg/MP)

Q = Intake flow rate (m^3/d)

The result is a flux in mass units, for the number-based value this result needs to be divided again by m_{MP}*10^{-6} [kg/particle]. The assumptions and the results are summarised in Table 6.1. About 43 kg of MP pass the system daily, or 8.60*10^8 MP particles. By extension, an estimated 3 250 kg/d (≈ 1 000 ton MP/year) or 6.50*10^{10} particles/d pass through the total capacity of SWRO installations worldwide.

Table 6.1:
Overview of the assumptions, characteristics and calculated results with respect to the first estimations in terms of total plastic flux through a large-scale SWRO plant (Ashkelon, Israel).

Parameter	**Symbol**	**Value**	**Unit**	**Source**
MP concentration	C	1	particles/L	[6]
MP particle mass	m_{MP}	0.005	mg/particle	[6, 11, 19]
Ashkelon intake flow	Q	860 000	m^3/d	[43]
Worldwide intake flow	Q	65 000 000	m^3/d	[79]
Results (Eq. 6.1)				
1 installation (Ashkelon)	-	43	kg/d	-
	-	8.60*10^8	particles/d	-
Worldwide	-	3 250	kg/d	-
	-	6.50*10^{10}	particles/d	-

The above calculations are followed by some remarks. First of all, during the operation there is a potential stream of MP particles passing through the system daily that is in the order of magnitude of kilograms. Even if the estimated MP concentration in the seawater taken in by the pumps is an overestimation, this still might lead to a high amount in terms of number of particles because of the low weight of an MP particle. Importantly, the hazards associated with MP particles in a marine environment (cfr. Section 2.1.2) are typically related to the presence of a certain amount of particles instead of its total mass. These numbers are logical given the high flux of seawater through an SWRO system. Secondly, as stated before, it is clear that there is little information on particular MP concentrations and their vertical distribution so far, few datasets to back hypotheses and a lot of uncertainty associated with such estimations. However, this reveals that there is some potential towards MP removal, given that this plastic flux passes the system anyway. Therefore, the final part of this research consists of more detailed mass balance calculations including the experimental results on removal effiencies of pretreatment processes.

6.2 SWRO Mass Balance

6.2.1 General Assumptions

The plastic flux will be further studied by means of simulating various scenarios to explore the potential for separation and removal of MP from an SWRO system. For this, the general system present in Figure 6.1 is considered. The intake pumps send a daily volume of seawater through the system consisting of the two conventional pretreatment steps (DMF and MF) and the RO modules themselves. Each step has their specific flow rates, removal efficiency and backwash efficiency (i.e. the fraction flushed out of the filtration system). Both efficiencies of the DMF and MF step are derived from the experimental results and are summarised in Table 6.2. Other characteristics present in Figure 6.1 are derived from literature. All simulation parameters are listed in Table 6.3. The goal of the simulations is to predict the fate of the MP passing through an SWRO system. In order to quantify this, the concentrations of MP in each reject stream and the total mass and number of MP that is separated from the incoming seawater are calculated.

Table 6.2:
Summary of the experimental results on DMF and MF as pretreatment step in SWRO. (SD = standard deviation)

Parameter	Symbol	Value	SD	Unit
DMF				
Removal efficiency	E_{DMF}	32	± 13	%
Backwash efficiency	η_{DMF}	99.994	± 0.002	%
MF				
Removal efficiency	E_{MF}	39	± 16	%
Backwash efficiency	η_{MF}	99.990	± 0.004	%

Table 6.3:
Overview of all input parameters that make up the studied system of an SWRO installation used in the simulation calculations (Figure 6.1).

Parameter	Symbol	Value	Unit	Source
Ingoing flow rate	Q_{in}	860 000	m^3/d	[43]
Recovery DMF	f_{DMF}	94	%	[61]
Recovery MF	f_{MF}	98	%	[57]
Recovery RO	f_{RO}	50	%	[46–48]
MP removal efficiency DMF	E_{DMF}	32	%	Section 5.3.2
MP removal efficieny MF	E_{MF}	39	%	Section 5.3.3
MP backwash efficiency DMF	η_{DMF}	99.994	%	Section 5.3.2
MP backwash efficiency MF	η_{DMF}	99.990	%	Section 5.3.3
MP particle mass	m_{MP}	0.005	mg/MP	[6, 11, 19]
Seawater density	ρ_{SW}	1027	kg/m^3	[78]
RO brine density	ρ_B	1054	kg/m^3	[78]

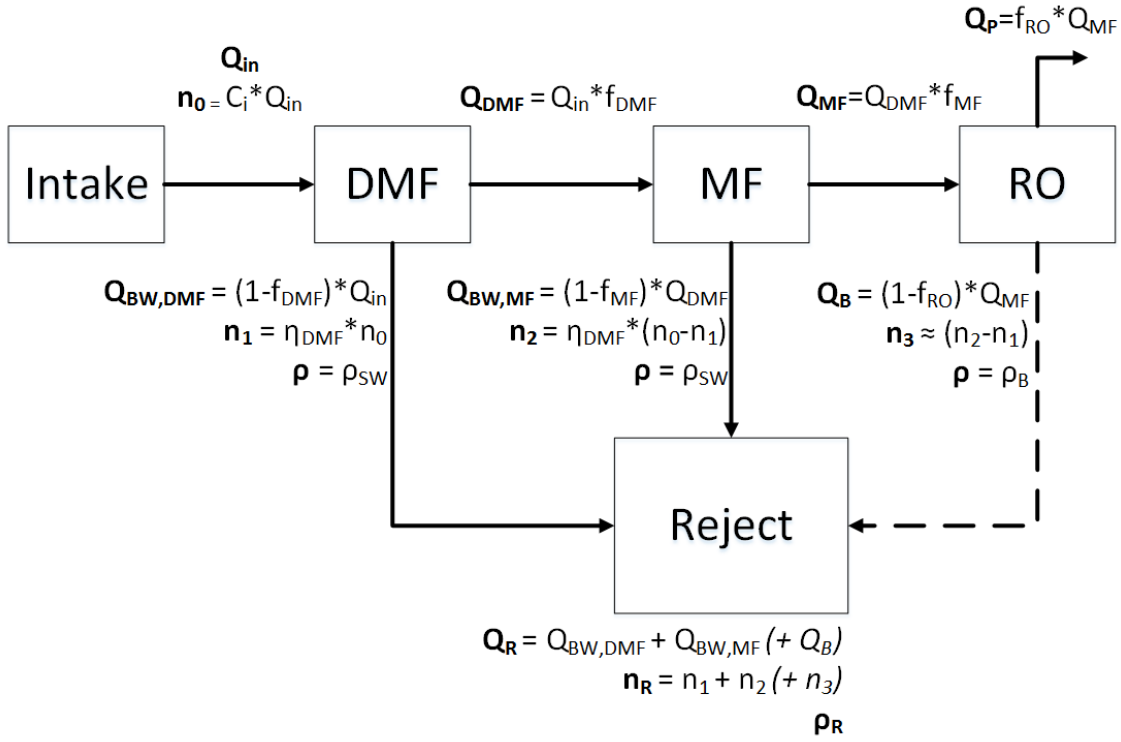

Figure 6.1: *This graphic illustrates the system studied during the final simulation calculations. The dashed line from RO to reject reflects one of the variable parameters where the mixing of the RO reject stream with the other reject streams from the pretreatment steps is optional. n_0 = ingoing MP (MP); n_1 = MP in the DMF backwash stream (MP); n_2 = MP in the MF backwash stream; n_3 = MP in the RO reject stream (MP); n_R = total MP in the mix of reject streams (MP); Q_{DMF} = average flow rate after the DMF step, including the volume needed for backwash (m^3/d); $Q_{BW,DMF}$ = DMF backwash flow rate (m^3/d); Q_{MF} = average flow rate after the MF step, including the volume needed for backwash (m^3/d); $Q_{BW,MF}$ = MF backwash flow rate (m^3/d); Q_P = RO permeate flow rate (m^3/d); Q_B = RO reject stream (m^3/d); Q_R = total flow rate of the mix of reject streams (m^3/d); ρ_R = density of the resulting mixture (kg/m^3). All remaining parameters are defined in Table 6.3.*

The construction of this simulation is based on some assumptions. First of all, when a plastic type enters the system, the density is the average of a virgin plastic particle (cfr. Table 2.1). In other words, the effect of biofouling on a particle's density is ignored. Even though the effect itself has been observed in previous studies, the experimental set-up during this research (Section 5.2) does not allow to accurately quantify this effect of biofouling on a plastic particle's density in such a way that a significant effect on its floating behaviour in seawater can be assumed. Secondly, there is a difference in the removal efficiency of a unit step and its backwash efficiency. This implies a significant fraction of the MP remains on the filter material or elsewhere in the system. This phenomenon is considered irreversible so these MP cannot be retrieved in the reject streams any more. The reject streams from each unit process are assumed to be easily combined and mixed within the SWRO installations. Finally, only the DMF and MF pretreatment steps are considered as important hotspots for separation and concentration of MP from the incoming seawater. Other

typical steps such as screening, with mesh sizes in the range of 1 to 10 mm [60, 63], are not included in the mass balance of the considered system.

6.2.2 Scenario Simulation

The different scenarios in these simulation calculations are the result of the variation of 3 parameters: the ingoing MP concentration, the composition of the ingoing MP flux and the fact whether the brine from the RO modules is being mixed with the pretreatment rejects:

1. **MP concentration**: As mentioned before, Li et al. [6] collected results from sampling studies (range: 0.1-10 MP/m^3), yet only two of these include the smaller fraction of the MP range while most others are limited to sampling plastic fragments larger than 1 mm. These two studies report 4 594 and 16 000 particles/m^3, respectively [20] and [21]. For this reason, the concentrations fed to the SWRO intake are selected as follows: (1) a concentration of 0.1 MP/m^3 and (2) 10 MP/m^3, corresponding with the range found in studies using sampling methods that ignore the smaller fraction of MPs and; (3) 48.8 MP/m^3, an average concentration of MP in seawater as predicted for 2100 by modeling research in Everaert et al. (2018) [17]; and (4) a concentration of 1 000 MP/m^3 (1 MP/L), which is more in line with the studies in Li et al. (2016) [6] with finer sample collection methods [20, 21] in coastal areas, where the intake system of an SWRO installations is also located. This third assumption is also supported by the expert knowledge of Prof. Dr. Colin Janssen (University of Ghent).

2. **Plastics composition**: In terms of distribution of plastic types in the ingoing seawater stream Q_{in}, two different situations are sketched. In the first one (situation A), the distribution reflects the worldwide production of plastics (cfr. Table 2.1) as is suggested by Andrady (2011) [1]. The second situation (situation B) is based on the findings in Reisser et al. (2015) where a sampling study of the top 5 meter of the water in the North Atlantic reveals the following distribution of MP in open sea: 84.7% of PE and 15.3% of PP, both a plastic type that has a lower density than seawater [19]. This second situation is included because intake systems of SWRO installations are typically situated within this top layer (cfr. Section 2.2.4).

3. **Mixing RO brine**: In Section 5.1, there is already an attempt to assess the application of the denser RO brine to improve the efficiency of separating MP from the reject streams that results from SWRO pretreatment steps. This will be repeated here to evaluate the effect during the simulation calculations, by choosing whether

the reject streams $Q_{BW,DMF}$ and $Q_{BW,MF}$ are mixed with the RO brine Q_B. This option is represented as a dashed line in Figure 6.1.

The final result is the amount of MP (number-based and mass-based) that would be floating on top of the reject streams (i.e. whose density is higher than the waste stream itself) and which form a potential hotspot for a relatively easy removal from these streams. Table 6.4 provides an overview of the different scenarios and their corresponding outcomes.

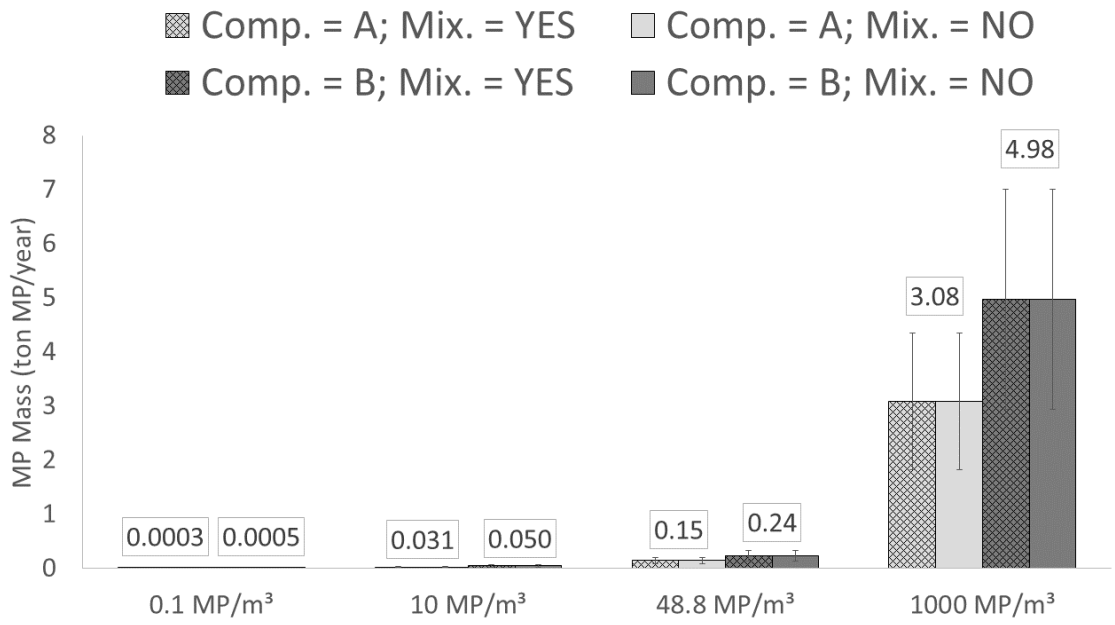

Figure 6.2: *This graphic presents the final outcome of the simulation calculation as they are listed in the final 2 columns of Table 6.4 in order to visualise the difference in effect of every variable parameter. The result is the estimated amount of MP to be afloat in the reject stream for every scenario (ton MP per year). The different scenarios are presented in order from left to right (scenario 1 through 16). The scenarios with the same ingoing MP concentration are grouped together. Legend: Comp. = Composition (Situation A or B); Mix. = Mixing of RO brine (YES or NO). The error bars are the standard deviation as a result of the uncertainty on the experimental removal and backwash efficiencies. Only 8 values are displayed instead of all 16, as the parameter of mixing RO brine with the pretreatment reject streams does not influence the result in this simulation, so both bars with and without cross pattern lead to the same result.*

The largest difference in results depends on the ingoing concentration. It has been mentioned from the beginning of this paper that there are still many uncertainties in terms of the extent of marine MP pollution, which is reflected in the 10 000-fold difference between the first and the last scenarios. If the MP pollution problem is overestimated, and concentrations are in the order of magnitude of 0.1 MP per cubic meter of seawater, then it is estimated that the total amount of recovered MP does not exceed 1 kilogram on a yearly basis. If the ingoing concentrations are assumed to be higher, e.g. as a result of finer sampling methods or in coastal/estuary areas, then the yearly recovered amount of MP results as high as the order of magnitude of 1 ton of MP: 5 ± 2 ton MP/year in the "best-case" scenario.

The 2 situations in terms of plastic composition (situations A or B) determine the eventually recovered (i.e. by density separation) fraction of the MP that end up in the final waste stream. In situation A, about 62% of the incoming plastic is lighter than seawater while in situation B, based on an analysis of sampled MP in the upper 5 meter layer, all plastic types that occur are lighter than seawater.

The final parameter is the mixing of RO brine with the other reject streams in order to increase the density of the reject mixture for more efficient density separation. However, it turns out that for the given incoming MP streams, there is no effect of this parameter on the result in any scenario.

Table 6.4:
This table lists all the simulated scenarios in one large-scale SWRO installation as a result of varying 3 parameters: ingoing MP concentration ("Concentration"), plastics composition ("Comp.") and mixing of the RO brine ("Mixing") with the pretreatment rejection streams. In the remainder of the table, an overview of the calculated results for every scenario is given based on the system in Figure 6.1. For all reject streams, the resulting concentration of MP is given as well as the total amount of MP isolated from the incoming stream of seawater Q_{in}. This is expressed as a mass of MP (m_{sep}, on a daily as well as a yearly basis). All calculated results are reported with their corresponding standard deviations, which result from the standard deviation of the experimental outcomes for DMF and MF backwash and removal efficiencies. SD = standard deviation.

#	**Concentration** (MP/m^3)	**Comp.** (-)	**Mixing** (-)	C_{DMF} (MP/m^3)	SD (MP/m^3)	C_{MF} (MP/m^3)	SD (MP/m^3)	m_{sep} (kg MP/d)	SD (kg MP/d)	m_{sep} (ton MP/yr)	SD (ton MP/yr)
1	0.1	A	Yes	0.5	±0.2	0.00012	±0.00005	0.0008	±0.0003	0.0003	±0.0001
2	0.1	A	No	0.5	±0.2	0.00012	±0.00005	0.0008	±0.0003	0.0003	±0.0001
3	0.1	B	Yes	0.5	±0.2	0.00012	±0.00005	0.0014	±0.0006	0.0005	±0.0002
4	0.1	B	No	0.5	±0.2	0.00012	±0.00005	0.0014	±0.0006	0.0005	±0.0002
5	10	A	Yes	53	±22	0.012	±0.005	0.08	±0.03	0.03	±0.01
6	10	A	No	53	±22	0.012	±0.005	0.08	±0.03	0.03	±0.01
7	10	B	Yes	53	±22	0.012	±0.005	0.14	±0.06	0.05	±0.02
8	10	B	No	53	±22	0.012	±0.005	0.14	±0.06	0.05	±0.02
9	48.8	A	Yes	258	±106	0.06	±0.02	0.41	±0.17	0.15	±0.06
10	48.8	A	No	258	±106	0.06	±0.02	0.41	±0.17	0.15	±0.06
11	48.8	B	Yes	258	±106	0.06	±0.02	0.67	±0.27	0.3	±0.1
12	48.8	B	No	258	±106	0.06	±0.02	0.67	±0.27	0.3	±0.1
13	1 000	A	Yes	5 283	±2 164	1.2	±0.5	9	±3	3	±1
14	1 000	A	No	5 283	±2 164	1.2	±0.5	9	±3	3	±1
15	1 000	B	Yes	5 283	±2 164	1.2	±0.5	14	±6	5	±2
16	1 000	B	No	5 283	±2 164	1.2	±0.5	14	±6	5	±2

CHAPTER 7

DISCUSSION

7.1 Experimental research

The first part of the experimental research focusses on the influence of biofouling on the density of a plastic particle. First of all, the method to determine the density is not accurate enough to follow up the progress of the particles' density through time. All experiments on PE beads (both Biofouling 1 and Biofouling 2, with different conditions) do not reveal a correlation between biofilm formation (measured by means of ATP concentration) and the particle density. The only experiment which gives an indication of this correlation between both, which has been observed before in previous research, is the one experiment on PP particles. This can be explained by the difference in density of the virgin plastic beads: the PE beads have a density of 0.98 g/cm^3, the PP beads only 0.90 g/cm^3. Because of this, the absolute difference between plastic density and biofilm density (1.14 g/cm^3, cfr. Section 2.1.3) is larger for the PP beads and an effect (i.e. an increase of density due to a higher degree of biofouling, as reflected in an increase in ATP concentration) can be observed more easily than for the heavier PE beads, whose density is closer to the biofilm's density.

The second part of the experimental research assesses the fate of MP in SWRO pretreatment processes. Table 6.2 summarises the removal and backwash efficiencies from the experimental set-ups for DMF and MF. Firstly, it is shown that both pretreatment steps are very efficient in terms of removal of MP from the incoming (sea)water stream, both for PE in the size range of 90-106 μm (quantitatively) and of 10-45 μm (qualitatively). MP present in the incoming seawater of an SWRO installation do not reach the RO modules itself. Instead, they are held up in the pretreatment process. Also, the analysis of the vertical distribution of MP in the DMF columns show no sign of breakthrough: over 90% of the MP present in the filter material is retrieved in the top 2 segments (out of 10 = top 20% of the column). Lastly, both DMF and MF were executed in a first series with tap water (DMF1 and MF1). Later they were performed with seawater (DMF2 and MF2) to better simulate a realistic SWRO scenario (cfr. Table 4.3). However, given the uncertainty on the measurements resulting from

these experiments, a difference in outcomes cannot be stated between both types of feed water.

The goal of this thesis research is to point out hotspots where MP are concentrated throughout the system in order to form a basis for further research on methods to remove MP from these concentrated reject streams. In this study, the resulting backwash efficiencies allow to further trace the MP in the described system as they end up in the reject streams of the two studied pretreatment steps. The two studied setups result in backwash efficiencies of 32% and 39%, for DMF and MF respectively. The DMF pretreatment step typically precedes the MF step and it is shown that a DMF step has a high removal efficiency of MP, so only a very small fraction of the incoming MP will reach as far as the MF units. As a consequence, the majority of the recovered MP will be found in the DMF reject stream. In practice, this reject stream is typically discharged again in the sea or the ocean from where the original intake water is drawn.

7.2 Simulations

The simulation calculations indicate a broad range of results in terms of removal potential of MP in this way. On the one hand, there are the most conservative scenarios in which only a fraction floats on top of the reject streams and the concentrations are low: 0.1 to 10 MP/m^3. These concentrations are typically the result of sampling studies in open sea. Based on these conservative parameters, the removal of potential of MP in this process is estimated to range from 0.3 kg to 50 kg per year, for one large-scale SWRO installation. On the other hand, when incoming MP concentrations are higher, as they are reported in coastal and estuary areas or as they are estimated to increase in the future, this potential is estimated to range from 150 kg to as high as 5 tonnes of MP per year, for one large-scale SWRO installation. In terms of MP, this is a very significant amount that can potentially be removed from sea water in existing installations. In order to put these results in some context, the worldwide production of plastics exceeds 300 million tonnes/year (cfr. Figure 2.1). Eriksen et al. (2014) [22] report an estimate of the worldwide MP pollution: 268 940 tonnes or 5.25 trillion plastic particles. Andrady (2017) [3] estimates a yearly input of 4.8-12.7 million tonnes of waste plastics ending up as litter in the oceans. These numbers vary strongly but the order of magnitude is clearly higher than what is calculated in this study in terms of removal. However, as a flux of plastic particle passes through such large-scale installations either way, these findings indicate the potential to remove a fraction of the MP pollution, albeit a small one.

Apart from the ingoing concentration and the composition of the ingoing MP in terms of polymer type, the assessment of the application of RO brine is also included in this theoretical approach. This brine, which is seawater of higher salt content, is considered a waste stream. Therefore, it is included in this study to evaluate its role in improving the separation efficiency of MP from the reject streams. The results are negative, as this does not affect the end result of the simulations. This can be explained by the relatively small increase in density of the mixed reject streams when this is compared with the density ranges of typical polymers on which these simulation calculations also have been based.

Either way, it is shown that these processes offer potential to collect, concentrate and, possibly, remove a certain flux of MP that passes through the SWRO system anyway. From here on, there are two main issues that need further research and discussion: (1) What is the actual intake of MP by SWRO installations? Are the assumptions in this study reasonably deduced from the current knowledge on occurrence of MP in the marine environment? (2) After pointing out MP hotspots in SWRO installations, how can they be removed from the process streams?

7.3 Future Research

This study achieves to determine removal and backwash efficiencies of MP in conventional SWRO pretreatment steps. However, the chosen spike for quantification is limited to a size range around 100 μm, while a quantitative indication is observed for smaller MP too (10-45 μm). A reproduction of these results for a broader range of MP, especially in the size range of 1-100 μm, will be particularly interesting. This allows a more solid quantification of the fate of the entire size range of MP in these unit processes. This can also lead to a more accurate prediction of the amount of MP that can potentially be removed from the reject streams.

During the experimental research, the MP are limited to spherical particles, as these products are readily available if one wishes to use standardized MP to facilitate the counting procedure. However, many studies report a significant fraction of plastic fibres as part of the MP occurring in marine environments. In Michielssen et al. (2016), for example, it is observed that plastic fibres are generally removed less efficiently than beads. This possible difference in behaviour and fate in the systems studied here is an interesting path for subsequent analysis. Just as described in the previous paragraph, this will allow a better quantification of the fate of the entire range of MP occurring in the natural environment.

Finally, in the simulation calculations, two variable parameters strongly influenced the end result. Both parameters have been selected to vary as there is little certainty about their true nature. The ingoing concentration and the composition of the plastic flux is crucial in making a better prediction of the total amount of MP that enters an SWRO installation and the total amount of 'end product', i.e. the recovered mass of MP. Especially knowledge on the vertical distribution of MP in the top layer of the water mass is crucial in estimating the order of magnitude of the plastic flux through SWRO installations. Are the ingoing MP predominantly PE and PP? Can their concentration at a certain depth be predicted by sampling at the surface? In relation to this, experimental studies to more accurately quantify the rate of biofouling and, subsequently, the rate of density change of a certain plastic particle are an interesting addition to the story of MP marine pollution. The type of MP and their density, once they end up in the indicated reject streams, are an important characteristic to further study their removal potential: what technologies are available and how can they be implemented in a reasonable way?

CHAPTER 8

CONCLUSION

MP pollution of the marine environment is a widespread and globally observed phenomenon. SWRO installations process high flow rates of seawater (up to the order of magnitude of 100 000 m^3/d) for the production of drinking water. At the same time, MP that are present in this processed seawater pass through the same pretreatment steps as the seawater. This study has investigated the fate of MP during these steps: both DMF and MF retain over 99.9% of the incoming MP in the bench-scale set-ups. At the same time, respectively 32% and 39% of the ingoing flux is washed out again during the backwash procedures. In this way, a fraction of the MP taken in by such installations eventually ends up in a reject stream of the DMF pretreatment step which is of lower total volume than the original polluted seawater and, consequently, of a higher concentration of MP.

These findings reveal a potential for removal of this plastic flux from the SWRO process. The most conservative approach results in about $6 \cdot 10^8$ plastic particles (0.3 kg MP/year), while more optimistic scenarios result in up to $1 \cdot 10^{13}$ plastic particles (5 tonnes MP/year). Further research is challenged to investigate in which way this separation can take place: density separation, e.g. settling or centrifugation, or size separation, e.g. additional membrane filtration. The central question is how such a technology can be implemented within the existing systems in a reasonable and economical way, given the fact that there is no obvious (economical) production value. The concentration of MP in the reject streams, due to the normal operation of an SWRO installation, is one step. The next step is to remove this flux of MP in an effective way but with minimal additional costs for the operator.

If further research is able to pinpoint cost-effective and easily implemented technology to remove this MP flux before it is sent back into the marine environment, as is the case in conventional operation, this may offer an interesting pathway to remedy part of the MP pollution problem and produce an added value to the operation of SWRO installations in ecological terms.

BIBLIOGRAPHY

[1] A. L. Andrady, “Microplastics in the marine environment,” *Marine Pollution Bulletin*, vol. 62, no. 8, pp. 1596–1605, 2011.

[2] L. G. A. Barboza and B. C. G. Gimenez, “Microplastics in the marine environment: Current trends and future perspectives,” *Marine Pollution Bulletin*, vol. 97, no. 1-2, pp. 5–12, 2015.

[3] A. L. Andrady, “The plastic in microplastics: A review,” *Marine Pollution Bulletin*, vol. 119, no. 1, pp. 12–22, 2017.

[4] C. Stevens, *Polymeren: course notes*. 2015.

[5] R. Geyer, J. R. Jambeck, and K. L. Law, “Production, use, and fate of all plastics ever made,” *Science Advances*, vol. 3, no. 7, 2017.

[6] W. C. Li, H. F. Tse, and L. Fok, “Plastic waste in the marine environment: A review of sources, occurrence and effects,” *Science of the Total Environment*, vol. 566-567, pp. 333–349, 2016.

[7] J. G. B. Derraik, “The pollution of the marine environment by plastic debris: a review.,” *Marine Pollution Bulletin*, vol. 44, pp. 842–852, 2002.

[8] J. Lee, S. Hong, Y. K. Song, S. H. Hong, Y. C. Jang, M. Jang, N. W. Heo, G. M. Han, M. J. Lee, D. Kang, and W. Shim, “Relationships among the abundances of plastic debris in different size classes on beaches in South Korea,” *Marine Pollution Bulletin*, vol. 77, no. 1-2, pp. 349–354, 2013.

[9] R. C. Thompson, “Plastic debris in the marine environment: consequences and solutions,” *Marine Nature Conservation in Europe*, pp. 107–116, May 2006.

[10] UNEP, “Marine plastic debris and microplastics - Global lessons and research to inspire action and guide policy change.,” *United Nations Environment Program, Nairobi*, 2016.

[11] C. G. Avio, S. Gorbi, and F. Regoli, “Plastics and microplastics in the oceans: From emerging pollutants to emerged threat,” *Marine Environmental Research*, vol. 128, pp. 2–11, 2017.

[12] H. S. Auta, C. U. Emenike, and S. H. Fauziah, "Distribution and importance of microplastics in the marine environment: A review of the sources, fate, effects, and potential solutions," *Environment International*, vol. 102, pp. 165–176, 2017.

[13] J. Zhao, W. Ran, J. Teng, Y. Liu, H. Liu, X. Yin, R. Cao, and Q. Wang, "Microplastic pollution in sediments from the Bohai Sea and the Yellow Sea, China," *Science of the Total Environment*, vol. 640-641, pp. 637–645, 2018.

[14] R. C. Thompson, "Lost at Sea: Where Is All the Plastic?," *Science*, vol. 304, no. 5672, p. 838, 2004.

[15] C. M. Free, O. P. Jensen, S. A. Mason, M. Eriksen, N. J. Williamson, and B. Boldgiv, "High-levels of microplastic pollution in a large, remote, mountain lake," *Marine Pollution Bulletin*, vol. 85, no. 1, pp. 156–163, 2014.

[16] D. Eerkes-Medrano, R. C. Thompson, and D. C. Aldridge, "Microplastics in freshwater systems: A review of the emerging threats, identification of knowledge gaps and prioritisation of research needs," *Water Research*, vol. 75, pp. 63–82, 2015.

[17] G. Everaert, L. Van Cauwenberghe, M. De Rijcke, A. A. Koelmans, J. Mees, M. Vandegehuchte, and C. R. Janssen, "Risk assessment of microplastics in the ocean: Modelling approach and first conclusions," *Environmental Pollution*, vol. 242, pp. 1930–1938, 2018.

[18] A. Cozar, F. Echevarria, J. I. Gonzalez-Gordillo, X. Irigoien, B. Ubeda, S. Hernandez-Leon, A. T. Palma, S. Navarro, J. Garcia-de Lomas, A. Ruiz, M. L. Fernandez-de Puelles, and C. M. Duarte, "Plastic debris in the open ocean," *Proceedings of the National Academy of Sciences*, vol. 111, no. 28, pp. 10239–10244, 2014.

[19] J. Reisser, B. Slat, K. Noble, K. Du Plessis, M. Epp, M. Proietti, J. De Sonneville, T. Becker, and C. Pattiaratchi, "The vertical distribution of buoyant plastics at sea: An observational study in the North Atlantic Gyre," *Biogeosciences*, vol. 12, no. 4, pp. 1249–1256, 2015.

[20] J.-P. W. Desforges, M. Galbraith, N. Dangerfield, and P. S. Ross, "Widespread distribution of microplastics in subsurface seawater in the NE Pacific Ocean," *Marine Pollution Bulletin*, vol. 79, no. 1-2, pp. 94–99, 2014.

[21] S. Zhao, L. Zhu, T. Wang, and D. Li, "Suspended microplastics in the surface water of the Yangtze Estuary System, China : First observations on occurrence, distribution," *Marine Pollution Bulletin*, vol. 86, no. 1-2, pp. 562–568, 2014.

[22] M. Eriksen, L. C. M. Lebreton, H. S. Carson, M. Thiel, C. J. Moore, J. C. Borerro, F. Galgani, and P. G. Ryan, "Plastic Pollution in the World' s Oceans: More than 5 Trillion Plastic Pieces Weighing over 250 .000 Tons Afloat at Sea," *PLoS ONE*, vol. 9, no. 12, pp. 1–15, 2014.

[23] A. van Wezel, I. Caris, and S. A. Kools, "Release of primary microplastics from consumer products to wastewater in the Netherlands," *Environmental Toxicology and Chemistry*, vol. 35, no. 7, pp. 1627–1631, 2016.

[24] H. Lee, H.-J. Lee, and J.-h. Kwon, "Estimating microplastic-bound intake of hydrophobic organic chemicals by fish using measured desorption rates to artificial gut fluid," *Science of the Total Environment*, vol. 651, pp. 162–170, 2019.

[25] J. Wang, M. Wang, S. Ru, and X. Liu, "High levels of microplastic pollution in the sediments and benthic organisms of the South Yellow Sea , China," *Science of the Total Environment*, vol. 651, pp. 1661–1669, 2019.

[26] W. Courtene-Jones, B. Quinn, C. Ewins, S. F. Gary, and B. E. Narayanaswamy, "Consistent microplastic ingestion by deep-sea invertebrates over the last four decades (1976-2015), a study from the North East Atlantic," *Environmental Pollution*, vol. 244, pp. 503–512, 2019.

[27] J. F. Provencher, J. C. Vermaire, S. Avery-gomm, B. M. Braune, and M. L. Mallory, "Garbage in guano? Microplastic debris found in faecal precursors of seabirds known to ingest plastics," *Science of the Total Environment*, vol. 644, pp. 1477–1484, 2018.

[28] K. Tanaka, H. Takada, R. Yamashita, K. Mizukawa, and M.-a. Fukuwaka, "Accumulation of plastic-derived chemicals in tissues of seabirds ingesting marine plastics," *Marine Pollution Bulletin*, vol. 69, no. 1-2, pp. 219–222, 2013.

[29] E. R. Zettler, T. J. Mincer, and L. A. Amaral-zettler, "Life in the Plastisphere : Microbial Communities on Plastic Marine Debris," *Environmental Science & Technology*, vol. 47, pp. 7137–7146, 2013.

[30] L. Frère, L. Maignien, M. Chalopin, A. Huvet, E. Rinnert, H. Morrison, S. Kerninon, A.-l. Cassone, C. Lambert, J. Reveillaud, and I. Paul-Pont, "Microplastic bacterial communities in the Bay of Brest: Influence of polymer type and size," *Environmental Pollution*, vol. 242, pp. 614–625, 2018.

[31] C. D. Rummel, A. Jahnke, E. Gorokhova, D. Kühnel, and M. Schmitt-Jansen, "Impacts of biofilm formation on the fate and potential effects of microplastic in the aquatic environment," *Environmental Science and Technology Letters*, vol. 4, no. 7, pp. 258–267, 2017.

[32] S. Ye and A. L. Andrady, “Fouling of floating plastic debris under Biscayne Bay exposure conditions,” *Marine Pollution Bulletin*, vol. 22, no. 12, pp. 608–613, 1991.

[33] E. A. Pelve, K. M. Fontanez, and E. F. DeLong, “Bacterial succession on sinking particles in the ocean’s interior,” *Frontiers in Microbiology*, vol. 8, pp. 1–15, 2017.

[34] United Nations, “Stockholm Convention on Persistent Organic Pollutants (POPs),” 2001.

[35] T. Gouin, N. Roche, R. Lohmann, and G. Hodges, “A Thermodynamic Approach for Assessing the Environmental Exposure of Chemicals Absorbed to Microplastic,” *Environmental Science and Technology*, vol. 45, pp. 1466–1472, 2011.

[36] A. Bakir, S. J. Rowland, and R. C. Thompson, “Enhanced desorption of persistent organic pollutants from microplastics under simulated physiological conditions,” *Environmental Pollution*, vol. 185, pp. 16–23, 2014.

[37] S. W. Hermanowicz and J. J. Ganczarczyk, “Some Fluidization Characteristics of Biological Beds,” *Biotechnology and Bioengineering*, vol. 25, no. 5, pp. 1321–1330, 1983.

[38] M. Kooi, E. H. Van Nes, M. Scheffer, and A. A. Koelmans, “Ups and Downs in the Ocean: Effects of Biofouling on Vertical Transport of Microplastics,” *Environmental Science and Technology*, vol. 51, no. 14, pp. 7963–7971, 2017.

[39] K. L. Law, N. Maximenko, S. Morét-Ferguson, and E. Peacock, “Plastic Accumulation in the North Atlantic Subtropical Gyre,” *Science*, vol. 329, no. 5996, pp. 1185–1188, 2010.

[40] L. C. Woodall, A. Sanchez-Vidal, M. Canals, G. L. Paterson, R. Coppock, V. Sleight, A. Calafat, A. D. Rogers, B. E. Narayanaswamy, and R. C. Thompson, “The deep sea is a major sink for microplastic debris,” *Royal Society Open Science*, vol. 1, no. 4, 2014.

[41] D. Lobelle and M. Cunliffe, “Early microbial biofilm formation on marine plastic debris,” *Marine Pollution Bulletin*, vol. 62, no. 1, pp. 197–200, 2011.

[42] F. J. Millero, R. Feistel, D. G. Wright, and T. J. Mcdougall, “The composition of Standard Seawater and the definition of the Reference-Composition Salinity Scale,” *Deep-Sea Research I*, vol. 55, pp. 50–72, 2008.

[43] B. Sauvet-Goichon, “Ashkelon desalination plant: A successful challenge,” *Desalination*, vol. 203, pp. 75–81, 2007.

[44] L. F. Greenlee, D. F. Lawler, B. D. Freeman, B. Marrot, P. Moulin, and P. Ce, "Reverse osmosis desalination: Water sources, technology, and today's challenges," *Water Research*, vol. 43, no. 9, pp. 2317–2348, 2009.

[45] GWI, "Market-leading Analysis of the International Water Industry, Global Water Intelligence," tech. rep., 2012.

[46] S. S. Shenvi, A. M. Isloor, and A. F. Ismail, "A review on RO membrane technology: Developments and challenges," *Desalination*, vol. 368, pp. 10–26, 2015.

[47] A. R. D. Verliefde, P. Van der Meeren, and B. Van der Bruggen, *Solution-Diffusion Processes*, pp. 1–26. 2013.

[48] L. Malaeb and G. M. Ayoub, "Reverse osmosis technology for water treatment: State of the art review," *Desalination*, vol. 267, no. 1, pp. 1–8, 2011.

[49] Water Technology, "Sorek Desalination Plant." `https://www.water-technology.net/projects/sorek-desalination-plant/`, 2019. Accessed: 2019-03-30.

[50] Hyflux, "Pollution Control Study for Tuas Desalination and Power Plant Project," tech. rep., 2011.

[51] Suez, "Al Dur: seawater reverse osmosis desalination plant," tech. rep., 2019.

[52] M. Lambert, "AIChE Conference 2015," in *AIChE Conference 2015*, 2015.

[53] A. Belatoui, H. Bouabessalam, and O. Rouane, " Environmental effects of brine discharge from two desalination plants in Algeria (South Western Mediterranean)," *Desalination and Water Treatment*, vol. 76, no. January, pp. 311–318, 2017.

[54] Suez, "Bahía de Palma: Seawater Reverse Osmosis Desalination Plant Mallorca (Spain)," tech. rep., 2019.

[55] S. P. Kopko and L. K. Wang, "City of Cape Coral Reverse Osmosis Water Treatment Facility," tech. rep., Zorex Corporation, Cape Coral, 2012.

[56] World Bank, "Seawater and Brackish Water Desalination in the Middle East, North Africa and Central Asia: Final Report - Annex 5 - Malta," tech. rep., 2004.

[57] S. K. Al-Mashharawi, N. Ghaffour, M. Al-Ghamdi, and G. L. Amy, "Evaluating the efficiency of different microfiltration and ultrafiltration membranes used as pretreatment for Red Sea water reverse osmosis desalination," *Desalination and Water Treatment*, vol. 51, no. 1-3, pp. 617–626, 2013.

[58] A. R. Guastalli, F. X. Simon, Y. Penru, A. D. Kerchove, J. Llorens, and S. Baig, "Comparison of DMF and UF pre-treatments for particulate material and dissolved organic matter removal in SWRO desalination," *Desalination*, vol. 322, pp. 144–150, 2013.

[59] S. Jeong, G. Naidu, R. Vollprecht, T. Leiknes, and S. Vigneswaran, "In-depth analyses of organic matters in a full-scale seawater desalination plant and an autopsy of reverse osmosis membrane," *Separation and Purification Technology*, vol. 162, pp. 171–179, 2016.

[60] N. Voutchkov, "Considerations for Selection of Seawater Filtration Pretreatment System," *Desalination*, vol. 261, no. 3, pp. 354–364, 2010.

[61] W. J. Weber, *Physicochemical Processes for Water Quality Control*. Wiley-Interscience, illustrate ed., 1972.

[62] N. Sabiri, E. Monnier, V. Raimbault, A. Massé, V. Séchet, and P. Jaouen, "Effect of filtration rate on coal-sand dual-media filter performances for microalgae removal," *Environmental Technology*, vol. 38, no. 3, pp. 345–352, 2017.

[63] S. Jamaly, N. N. Darwish, I. Ahmed, and S. W. Hasan, "A short review on reverse osmosis pretreatment technologies," *Desalination*, vol. 354, pp. 30–38, 2014.

[64] M. R. Michielssen, E. R. Michielssen, J. Ni, and M. B. Duhaime, "Fate of microplastics and other small anthropogenic litter (sal) in wastewater treatment plants depends on unit processes employed," *Environmental Science: Water Research & Technology*, vol. 2, pp. 1064–1073, 2016.

[65] R. Sutton, S. A. Mason, S. K. Stanek, E. Willis-norton, I. F. Wren, and C. Box, "Microplastic contamination in the San Francisco Bay, California, USA," *Marine Pollution Bulletin*, vol. 109, no. 1, pp. 230–235, 2016.

[66] L. Yang, K. Li, S. Cui, Y. Kang, L. An, and K. Lei, "Removal of microplastics in municipal sewage from China's largest water reclamation plant," *Water Research*, vol. 155, pp. 175–181, 2019.

[67] E. A. Gies, J. L. LeNoble, M. Noël, A. Etemadifar, F. Bishay, E. R. Hall, and P. S. Ross, "Retention of microplastics in a major secondary wastewater treatment plant in Vancouver, Canada," *Marine Pollution Bulletin*, vol. 133, no. June, pp. 553–561, 2018.

[68] S. A. Carr, J. Liu, and A. G. Tesoro, "Transport and fate of microplastic particles in wastewater treatment plants," *Water Research*, vol. 91, pp. 174–182, 2016.

[69] T. M. Missimer and R. G. Maliva, “Environmental issues in seawater reverse osmosis desalination : Intakes and outfalls,” *Desalination*, vol. 434, pp. 198–215, 2018.

[70] D. Gille, “Seawater intakes for desalination plants,” *Desalination*, vol. 156, pp. 249–256, 2003.

[71] T. Pankratz, “Seawater desalination technology overview,” in *Presentation for Georgia Joint Comprehensive Study Committee, St. Simons Island, Georgia*, 2006.

[72] V. Bonnelye, M. A. Sanz, J.-P. Durand, L. Plasse, F. Gueguen, and P. Mazounie, “Reverse osmosis on open intake seawater: Pre-treatment strategy,” *Desalination*, vol. 167, pp. 191–200, 2004.

[73] M. Ahmed and R. Anwar, “An Assessment of the Environmental Impact of Brine Disposal in Marine Environment,” *International Journal of Modern Engineering Research*, vol. 24, pp. 2756–2761, 2012.

[74] R. Einav and F. Lokiec, “Environmental aspects of a desalination plant in Ashkelon,” *Desalination*, vol. 156, pp. 79–85, 2003.

[75] M. Ahmed, D. Hoey, M. R. Thumarukudyd, M. F. A. Goosen, M. Al-haddabi, and A. Al-belushi, “Feasibility of salt production Corn inland RO desalination plant reject brine : a case study,” *Desalination*, vol. 158, pp. 109–117, 2003.

[76] Aqua-Techniek, “Filtermedia for Water Treatment,” tech. rep., 2003.

[77] A. C. Mehner, “Multimedia and Ultrafiltration for Reverse Osmosis Pretreatment Aboard Naval Vessels,” *The University of Arkansas Undergraduate Research Journal*, vol. 11, 2010.

[78] F. J. Millero and F. Huang, “The density of seawater as a function of salinity (5 to 70 g/kg) and temperature (273.15 to 363.15 K),” *Ocean Science*, vol. 5, pp. 91–100, 2009.

[79] E. Jones, M. Qadir, M. T. H. V. Vliet, V. Smakhtin, and S.-m. Kang, “The state of desalination and brine production: A global outlook,” *Science of the Total Environment*, vol. 657, pp. 1343–1356, 2019.

APPENDIX A

SENSITIVITY ANALYSIS

METHOD 1

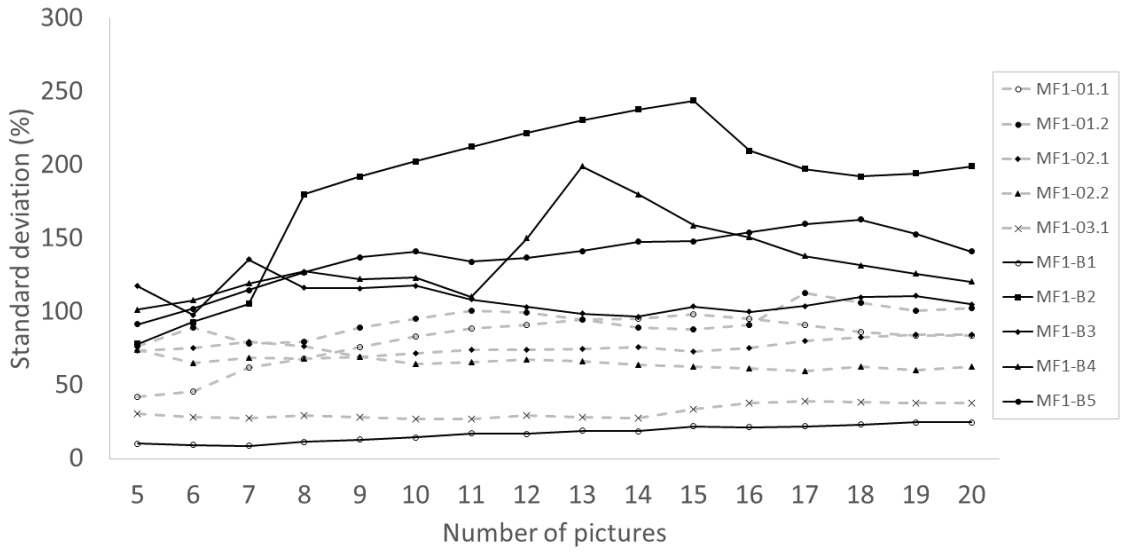

Figure A.1: *Evolution of the standard error on the estimated average of a filter in function of the amount of random pictures taken and processed. At every point, X random pictures of a certain filter are selected, the estimated amount of MP is calculated and averaged for the X pictures (X ranges from 5 to 20). The standard error is expressed as a relative value: it is every time normalised over the estimated average of a filter based on X pictures. The analysis is repeated 10 times with filters containing MP: 5 influent filters (MF1-01.1 until MF1-01.5, grey curves) and 5 backwash filters (MF1-B1 until MF1-B5, black curves).*